#1

EXPERIMENTAL STUDIES OF HANDWRITING SIGNALS

JOHN S. MACDONALD

Loan Copy Only

TECHNICAL REPORT 443

MARCH 31, 1966

MASSACHUSETTS INSTITUTE OF TECHNOLOGY
RESEARCH LABORATORY OF ELECTRONICS
CAMBRIDGE, MASSACHUSETTS

The Research Laboratory of Electronics is an interdepartmental laboratory in which faculty members and graduate students from numerous academic departments conduct research.

The research reported in this document was made possible in part by support extended the Massachusetts Institute of Technology, Research Laboratory of Electronics, by the JOINT SERVICES ELECTRONICS PROGRAMS (U.S. Army, U.S. Navy, and U.S. Air Force) under Contract No. DA36-039-AMC-03200(E); additional support was received from the National Science Foundation (Grant GP-2495), the National Institutes of Health (Grant MH-04737-05), and the National Aeronautics and Space Administration (Grant NsG-496).

MASSACHUSETTS INSTITUTE OF TECHNOLOGY

RESEARCH LABORATORY OF ELECTRONICS

Technical Report 443

March 31, 1966

EXPERIMENTAL STUDIES OF HANDWRITING SIGNALS

John S. MacDonald

This report is based on a thesis submitted to the Department of Electrical Engineering, M.I.T., August 24, 1964, in partial fulfillment of the requirements for the degree of Doctor of Philosophy.

(Manuscript received August 11, 1965)

Abstract

A system for measuring the displacement, velocity, and acceleration of handwriting movements has been developed. Samples of handwriting processed by this system indicate that the acceleration waveforms of uninterrupted handwriting approximate multilevel trapezoidal time functions.

Electronic simulation of the measured displacement, velocity, and acceleration waveforms of handwriting has been accomplished. The "handwriting" produced by the electronic simulator can duplicate uninterrupted handwriting with a high degree of accuracy. The simulator has been used both to generate samples of "handwriting" and to duplicate the handwriting of a number of subjects.

The simulator, in effect, represents a point mass driven by a trapezoidal "force" function. Although the biological system producing handwriting is highly complex, the motions involved can be duplicated with a high degree of accuracy in terms of an extremely simple mechanical model.

Some preliminary results have been obtained which are directed toward the establishment of relations between the model and the biological system responsible for handwriting. Possible applications of the techniques and apparatus developed in this report to problems of handwriting recognition and neurological studies are discussed.

TABLE OF CONTENTS

I. INTRODUCTION

1.1 BACKGROUND

In recent years, considerable interest has been aroused in the handwriting process. There are two main stimuli for this interest: The first is related to the need for recognition of handwriting by machine, and the second stems from an interest in the handwriting process as a means of studying properties and ailments of the biological system which produces it.

This report describes the procedure and some initial results of an investigation that sought to examine the handwriting process for its own sake. Motivation for this investigation is derived from both of the sources mentioned above, though chiefly from the realization that studies of handwriting signals have the potential to increase our knowledge of the function and organization of a biological system through the study of a common but sophisticated function of that system.

Cursive handwriting can be classed as a highly skilled process which is executed by means of a rapid sequence of motions. Such processes were studied as early as 1917 by Lashley.[9] It is widely accepted[10] among physiologists that the reaction time for tactile, kinesthetic or visual feedback is too long to enable these processes to be useful in the control of fast detailed motion. This reasoning, together with some experimental evidence, led Lashley to the postulation of some central nervous mechanism that fires with predetermined intensity and duration to control this type of motion.[10] In 1962, Denier van der Gon and his co-workers[1] suggested that handwriting might be controlled in this fashion. As a result of observations of acceleration while executing the cursive sequence lelelelele, they concluded that handwriting could be characterized by the timing of the force waveforms applied during the writing movement. Specifically they proposed that "the principles of fast uninterrupted handwriting are:

1. Fast handwriting is done without instantaneous position feedback.

2. Writing movements are caused by two independent groups of muscles. Each group, containing antagonistic muscles, governs motion to and fro in one direction. The directions of these two groups are more or less perpendicular to each other.

3. The antagonistic muscle groups alternately apply forces to hand and pencil. This system can be considered as a mass with some friction.

4. After its onset, the force rises (more or less linearly) to a certain fixed value and remains more or less constant. The duration of application of this force is related to the magnitude of a writing move. Thus different lengths of strokes in uninterrupted handwritten characters are caused by different time of application, and not by different magnitude of force."[1]

Denier van der Gon and his group built a simple electromechanical simulator based upon these principles, but their publication shows only three samples of handwriting which have been simulated. The samples published were taken from a large number of

written signatures. The simulated versions are remarkably good, but differ in detail from the originals. They were obtained by adjusting the simulator "in such a way that the results fitted in the group of written signatures."

The principles quoted above are simple and direct. The speculation that handwriting can be coded by consideration of the relative times of force reversal in the handwriting movements is particularly attractive. It leads one to ask: "If these researchers have done so well with a simple simulator constructed upon these principles, what modifications to the principles are required to obtain exact (i.e., with negligible error) duplication of a handwriting sample?" The research reported here commenced with the asking of this question.

1.2 SCOPE AND ORGANIZATION OF THE REPORT

We are concerned with the study of handwriting signals. Specifically, measurements are made of the vertical and horizontal projections of the displacement, velocity, and acceleration of the pencil point during handwriting and related movements. The results of these measurements are then used to achieve simulation of the writing motion and to establish a possible model for the handwriting process.

Experiments were initiated by designing and constructing an electronic simulator which was essentially equivalent to the simulator reported by Denier van der Gon. By using this simulator, it was quickly found that although one could make a "handwriting" that had all of the main features of the original, it was not possible to make exact duplicates by adjustment of the timing of the "force" signals.

As will be demonstrated through the simulations described in Section III, if one varies the "force" it is possible to obtain excellent duplication of handwriting. One can conclude from this that the output of the handwriting system can be modeled quite closely by the output of a second-order linear system driven by discrete force signals. This does not imply, however, that there is any similarity between the functional principles of the two systems. The outputs of two systems can be matched as closely as one pleases without shedding any light on the similarity of the systems. Putting it another way, two signals can be matched as closely as we please without any agreement between the analytic forms (even if they can be found) or the derivatives of the two signals. Thus we see that although the principles proposed by Denier van der Gon lead to a model capable of imitating handwriting, they do not necessarily lead to a model that is a direct analog of the system generating handwriting. The open question here is the degree of similarity between the principles of operation of the suggested model and those of the actual handwriting mechanism.

The measurements described in Section II show that if the effects of static friction and other minor effects are ignored, the acceleration waveforms can be approximated by trapezoidal waveforms (see Fig. 1). This result is in agreement with that of Smith[20] who discovered that the response of the human forearm following random input step commands was such that for high inertia and low damping the force waveform

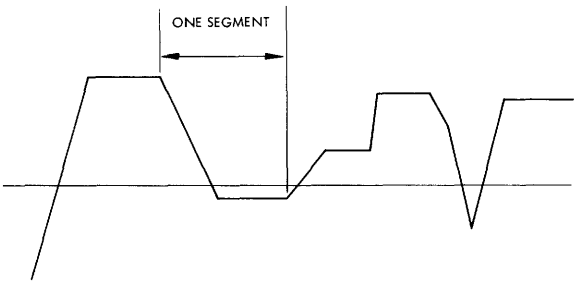

Fig. 1. Trapezoidal wave.

was trapezoidal. That is, the behavior was reminiscent of a bang-bang servo. Apparently, handwriting is controlled in similar fashion. The segments of the trapezoidal approximations to the acceleration waveforms assume several different levels as opposed to the two-level approximation assumed by Denier van der Gon.

The measurements and simulations presented here reveal that the acceleration, velocity, and displacement which constitute the output of the biological system that generates handwriting are closely approximated by the output of the systems described in Section IV. We make no assumptions about the origin of forces giving rise to the motion other than to say that they arise from the action of muscles. Which combinations of muscles are involved in any movement, or what is the nature of the associated nerve signals are questions which are not answered in this report. Possible methods for the solution of this problem will be discussed.

II. MEASUREMENT OF HANDWRITING SIGNALS

2.1 THE MEASURING SYSTEM

The system used to measure the displacement, velocity, and acceleration of handwriting movements consists of a device for transforming the motion of a pencil point into electrical signals proportional to the horizontal and vertical projections of the pencil displacement, together with the electronic apparatus necessary to take the first and second derivatives of the displacement signals. A block diagram is shown in Fig. 2.

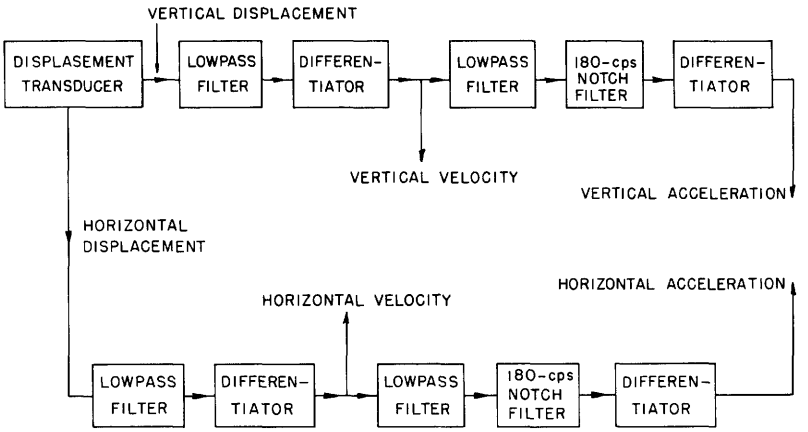

Fig. 2. Handwriting processor.

The displacement transducer produces electrical signals proportional to vertical and horizontal projections of the displacement of the pencil point. These signals are lowpass-filtered (the 3-db point of the filter is 100 cps) and differentiated to produce the velocity signals. The velocity signals are again lowpass-filtered (3-db point, 100 cps) and differentiated to produce the acceleration signal. The 180-cps notch filter was necessary to cut out the strong component at that frequency which was present in the laboratory at the time the measurements were made.

The measurement of acceleration by taking two derivatives of the projections of the displacement signal is preferable to direct measurement by, say, accelerometers attached to the hand or pencil because the coordinate system involved is fixed and simply and directly related to the writing itself.

The differentiator provides a transfer function

$$v_o = K\frac{dv_i}{dt}$$

over a minimum bandwidth of 500 cps, where v_i is the input voltage, v_o is the output voltage, and K takes on the values 0.08, 0.12 or 0.16, the value depending on the

settings of gain selector switches on the unit. Details can be found in Appendices of Reference 12.

The transducer used to create the displacement signals consists of an electrolytic tank approximately 4 feet square by 1 inch deep. The writing area is 4 inches by 8 inches in the center of the tank. The size of the tank relative to the writing area was chosen to yield a good approximation to uniform field patterns for all positions of the stylus. Four long electrodes are placed around the perimeter of the tank (see Fig. 3). The electrolyte is de-ionized water, and the electrodes are carbonized brass. The writing motion is executed by placing the pencil in the water through the 4 X 8 inch hole in the center of the tank cover. A current source supplies current through the pencil into the electrolyte.

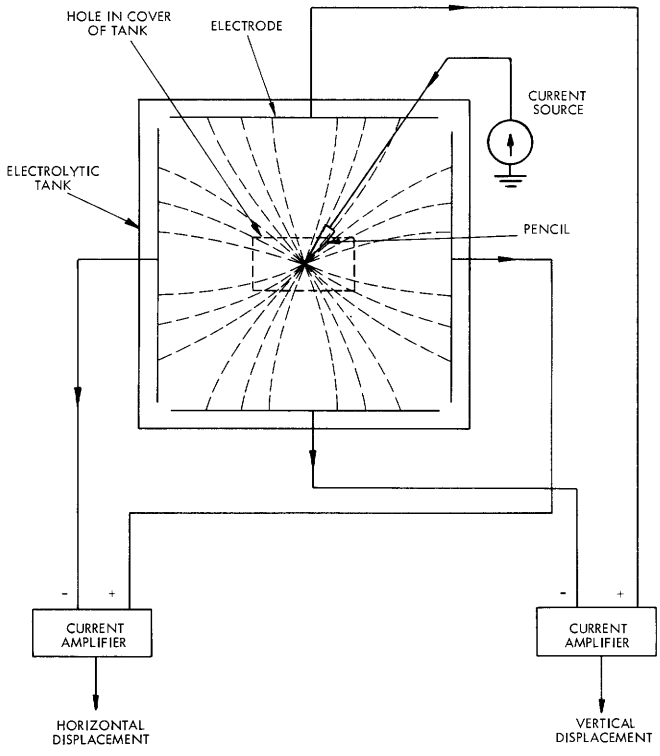

Fig. 3. Displacement transducer.

The displacement signals are obtained by subtracting the current reaching the top electrode from that reaching the bottom electrode to form the vertical displacement signal, and by subtracting the current reaching the right electrode from that reaching the left electrode to form the horizontal signal.

Several conductors were tried before water was chosen. Teledeltos paper and carbonized cloth were rejected because variations of the contact between the pencil and these conductors, as well as their basically discrete nature, caused excessive

noise in the acceleration signal. Admittedly, the use of a current source minimizes this problem, but the noise is not sufficiently low to permit two differentiations. Conducting glass has also been tried, and shows considerable promise. The sample obtained was too small and had conductivity too high to be useful with existing equipment, but being a smooth surface, it does not suffer from the noise problems occurring in other solid conductors.

The use of an all DC system was necessary because high-frequency (above 1 kc) carrier systems would lead to difficulties caused by the reactance of the electrolytic tank. Carriers of frequency low enough to circumvent the reactance problem are too close to the 100-cycle cutoff frequency required in the differentiation system, and would therefore interfere with the differentiation of the handwriting signals.

The electrolytic tank has the additional advantage that when the pencil is lifted, as in dotting an i or crossing a t, the displacement information is not lost as long as the pencil is not removed from the water. Its chief disadvantages are that it is cumbersome, and that waves on the water and polarization by the DC current tend to cause errors. Also, the subject doing the writing cannot assume a completely normal writing position because it is necessary to write on the bottom of the tank (approximately 1 inch below the plane upon which the hand must rest).

Some error occurs because of polarization of the electrolyte which creates a region of ion concentration around the pencil and upsets the uniform conductivity of the medium. Errors from this source are minimized by using de-ionized water and carbonized brass electrodes.[7]

The errors arising from waves on the water come from two sources: The first is from ripples caused by the motion of the pencil through the water. These ripples upset the symmetry of the current distribution around the pencil (see Fig. 3). Errors from this source are perceptible only in the second derivative of the handwriting signal. Measurements made by holding the pencil steady while blowing on the water to create waves like those caused by pencil motion indicate that the noise from this source is not objectionable, and can be essentially eliminated by using a needle-sized writing stylus insulated except for its tip (see Fig. 4). The second source of error resulting from wave motion is that caused by very slow movement of water. Error signals from this source are of very low frequency (around 1/10 cps), and are therefore of no consequence insofar as the derivatives are concerned. The slow wave motion does affect the displacement signal when long words are written, however, so before taking such a sample it is necessary to wait until the slow wave motion caused by leaning on the tank has subsided.

Figure 5 shows the results of a test conducted to determine the fidelity of the displacement output of this transducer. Figure 5a is the displacement curve actually executed by the pencil when writing in the tank. This record was obtained by attaching a piece of paper to the bottom of the tank. Figure 5b shows the output of the transducer which resulted.

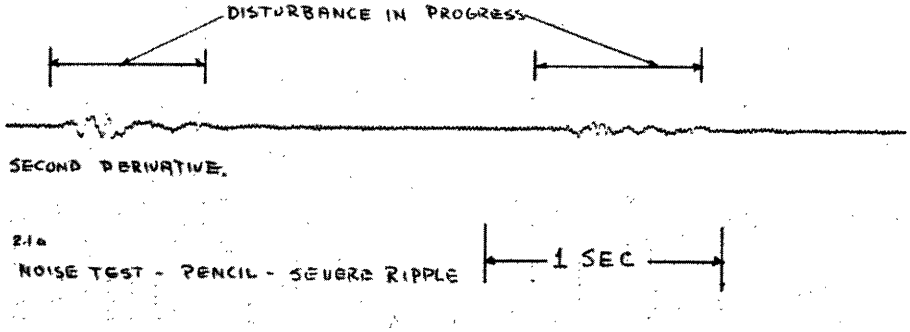

(a) PENCIL SEVERE RIPPLE

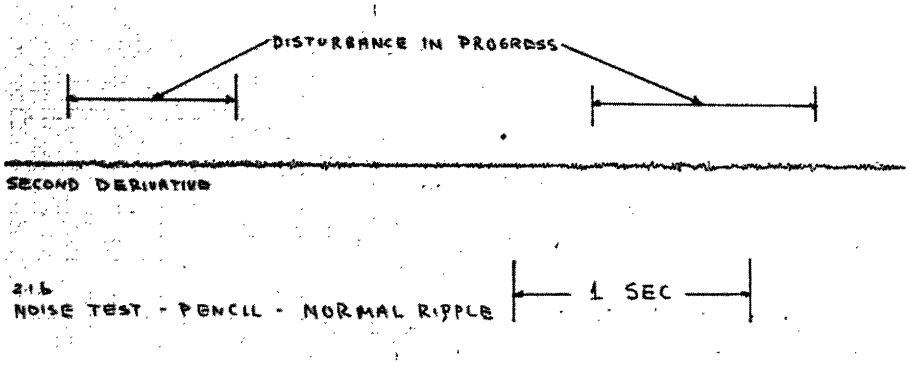

(b) PENCIL NORMAL RIPPLE

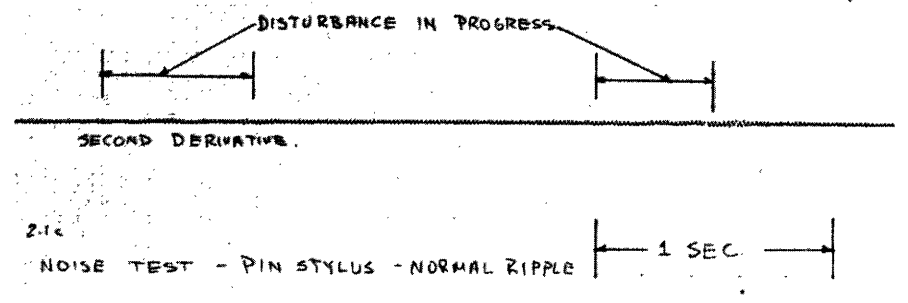

(c) PIN STYLUS NORMAL RIPPLE

Fig. 4. Ripple-noise tests.

(a) INPUT (b) OUTPUT

Fig. 5. Transducer input and output.

The accuracy of the electronic system used to derive the velocity and acceleration was tested by placing a signal of known form at the input to the system and observing the outputs. The test signal used is the step response of the circuit of Fig. 6a. The results displayed in Fig. 6b conform closely to the expected waveforms.

A further test of over-all system fidelity was conducted as follows: The pencil was drawn quickly against a rigid stop, thereby providing a step in the displacement waveform, a pulse in the velocity, and a doublet in the acceleration. The record of Fig. 7 shows the expected behavior.

In the experimental results to be considered, we shall be interested in matching the output waveforms with those generated by a simulator. The tests show that the fidelity of the outputs of the measuring system can be relied upon, at least to the extent required for a visual matching process.

2.2 EXPERIMENTAL ARRANGEMENT

The experimental arrangement used to conduct the measurements described here is diagrammed in Fig. 8. The outputs from the measuring system are fed into 6 channels of an FM magnetic tape recorder. These signals are thus made available for various kinds of processing that might be required later. In general, the signals are taken off the tape as required, and are fed into two Sanborn four-channel paper chart recorders. Time synchronization of the recorders, when two are used simultaneously, is provided in one of two ways: either a square-wave signal is recorded on one track of each recorder or the same information is recorded on one or two tracks of each recorder.

The x and y displacement signals are also fed into the horizontal and vertical inputs of a Tektronix Type 564 storage oscilloscope. This provides a temporary record of the writing during the course of the experiment. (Most subjects found it difficult to use the storage oscilloscope as a means of visual feedback because the image of their writing, appearing on the storage oscilloscope, was not in the place where they were accustomed to seeing it – on the surface upon which they were writing.)

When it is desired to display the output of the tape recorder on an oscilloscope,

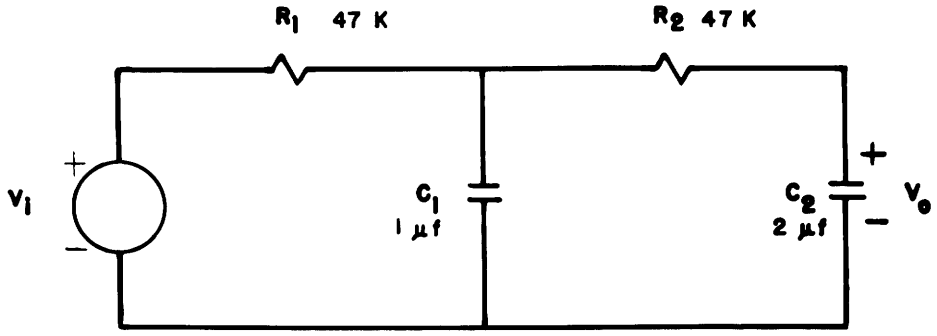

(a)

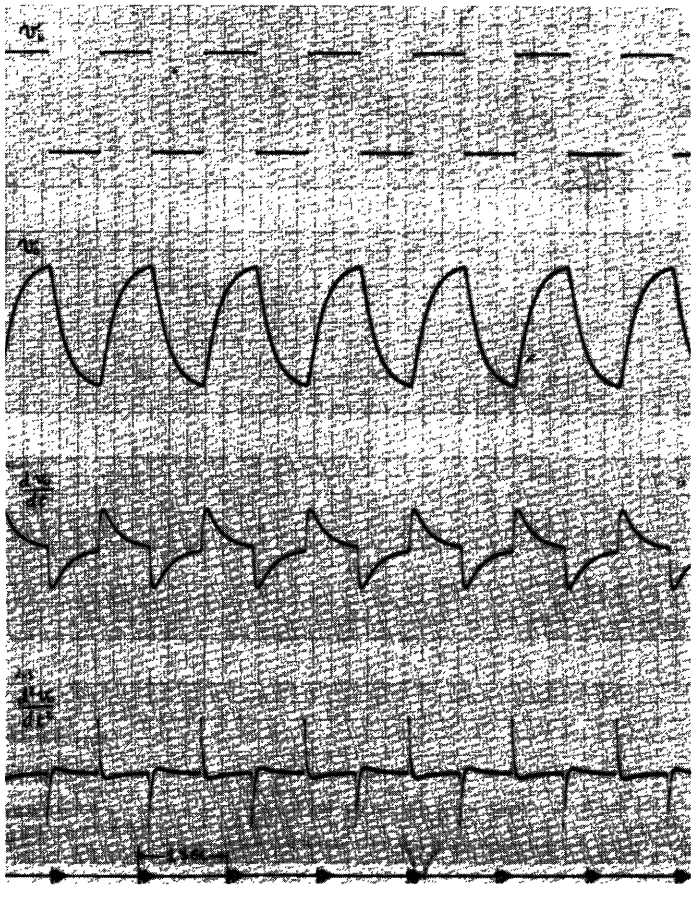

(b)

Fig. 6. Test of differentiators.

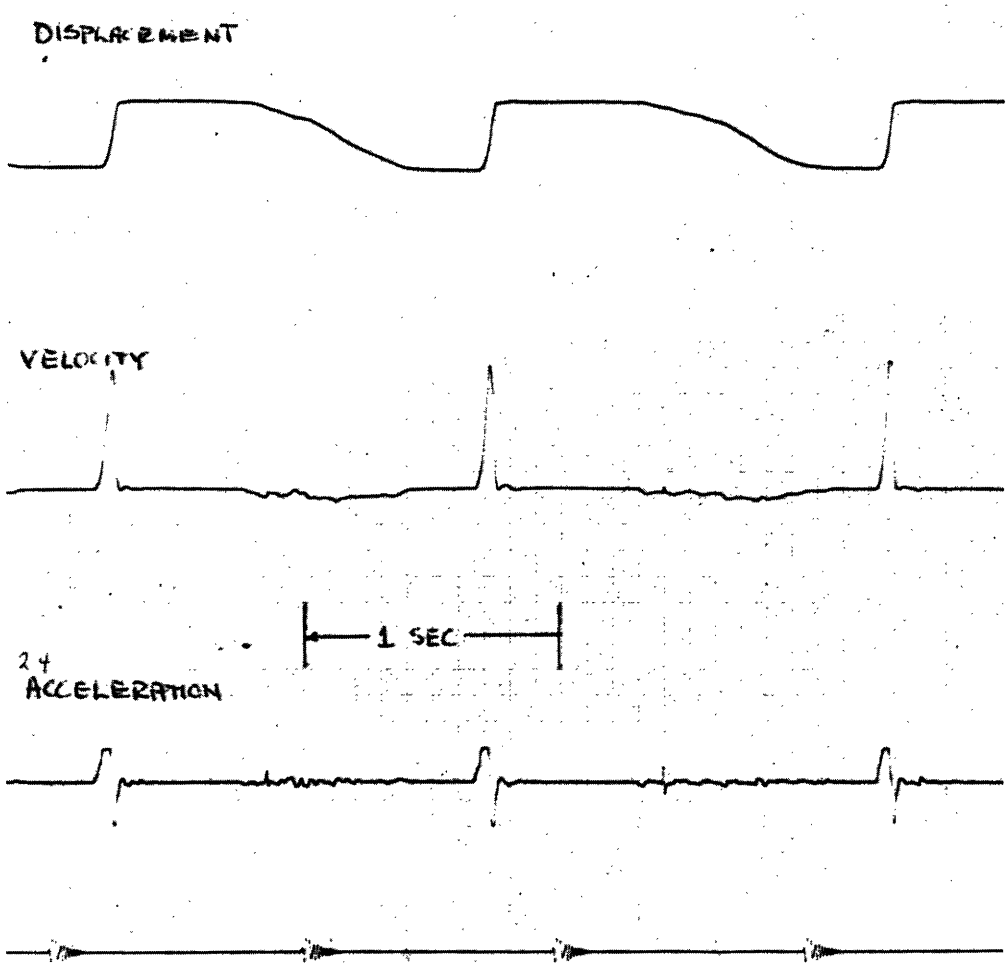

Fig. 7. Test of over-all system.

the signals are passed through 100-cps lowpass filters to eliminate some of the noise introduced by the tape recorder.

2.3 MEASUREMENT OF SIMPLE MOVEMENTS

Before the waveforms generated during actual handwriting could be studied, it was necessary to make measurements on simple motions such as repetitive to-and-fro or circular motions of the pencil. The effect on the acceleration waveform of static friction and noise introduced by the way in which the pencil is held are more easily evaluated from simple motions than the more complicated ones involved in actual handwriting.

Figure 9a shows a record of the displacement, velocity, and acceleration of a simple to-and-fro motion. The gross structure of the acceleration waveform is that of a square wave, but the fine structure is too large to be ignored. In particular, the large spikes that occur about midway between the obvious discontinuities in the waveform are seen to be the major component of this fine structure. (One of these is circled

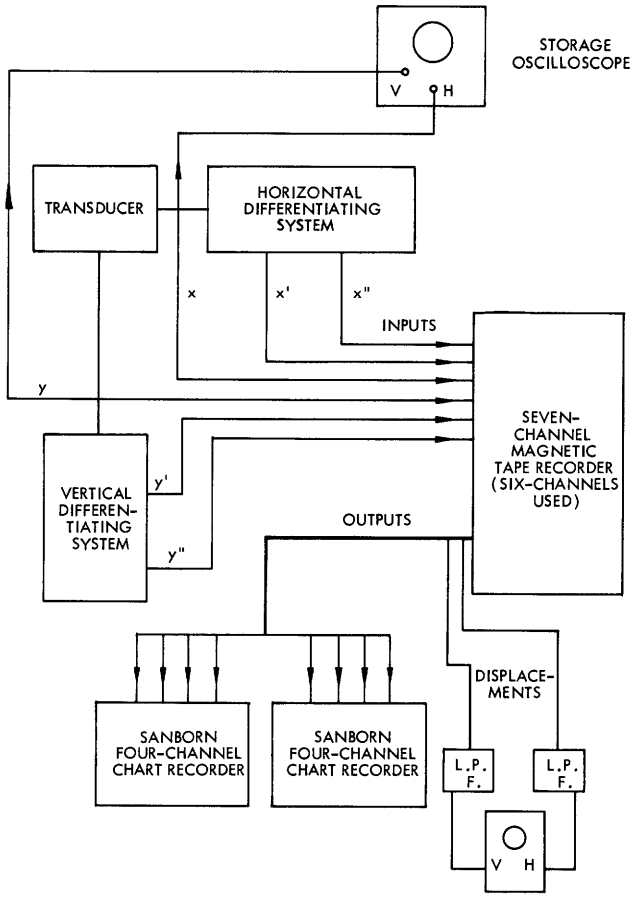

Fig. 8. Experimental arrangement.

in Fig. 9a.) These spikes line up with a plateau in the velocity waveform as expected. Moreover, these plateaus always occur at zero velocity, which suggests that the origin of these spikes is friction. This is easily verified by having the subject lift his pencil slightly off the bottom of the tank as he executes the motion. The resulting waveforms appear in Fig. 9b. A trapezoidal approximation is made to the last portion of the acceleration waveform.

The records of Fig. 10 show that the spikes referred to above arise from static friction. These records are the vertical projections of rotary motion where, although the vertical velocity is going through zero, the actual motion does not stop. The absence of spikes in the acceleration waveform of Fig. 10a, where the pencil was on the bottom, indicates that static friction is the cause of the spikes of Fig. 9a. Figure 10b shows the vertical component of rotary motion with the pencil lifted off the bottom. The same subject (EGB) made all of the records shown in Figs. 9 and 10.

Figure 11 shows the effect of static friction very dramatically. This record is from a different subject from the one responsible for Fig. 9, and the motion is left-right about the wrist joint. In Fig. 11b, the pencil was lifted off the bottom.

Figure 12 displays the displacement, velocity, and acceleration of vertical finger

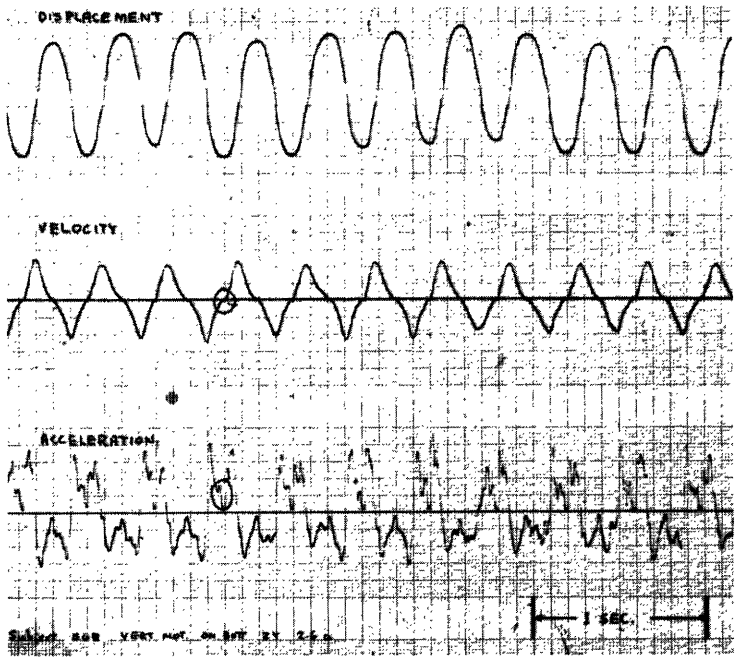

(a) PENCIL ON BOTTOM

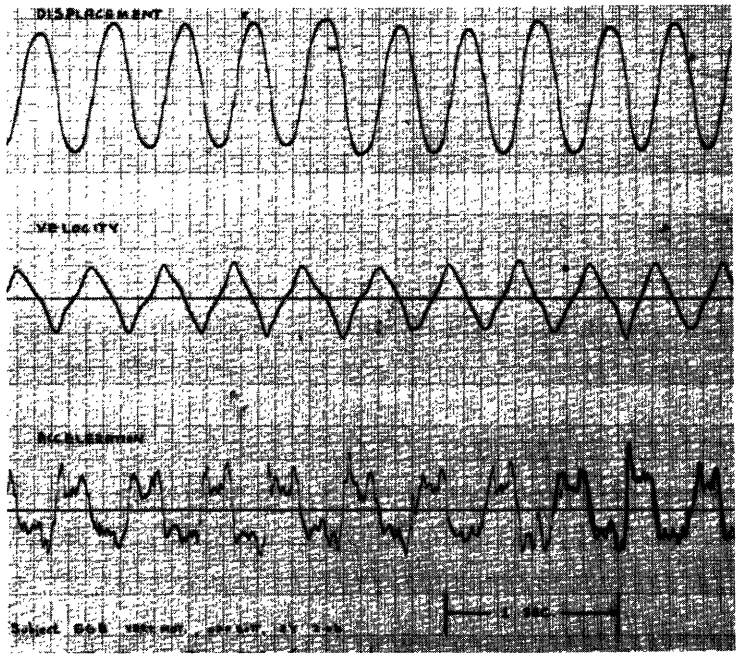

(b) PENCIL OFF BOTTOM

Fig. 9. Vertical motion – effect of friction.

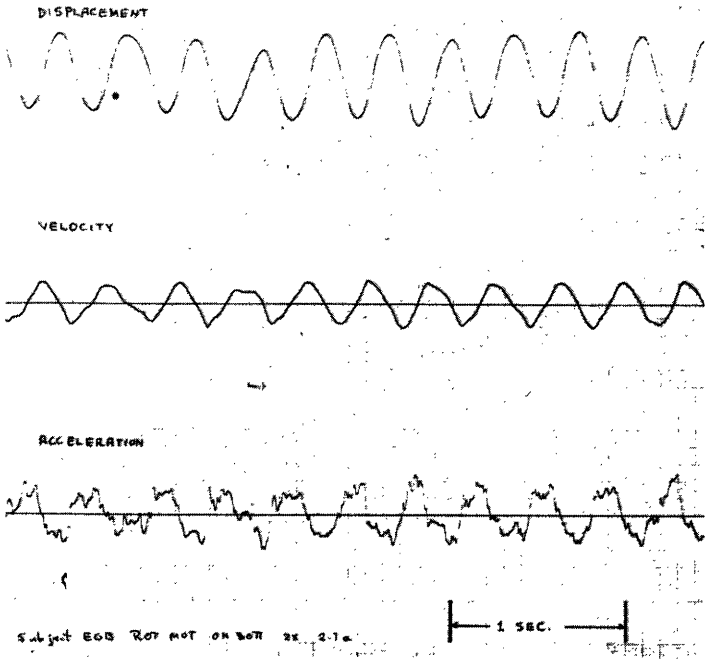

(a) PENCIL ON BOTTOM

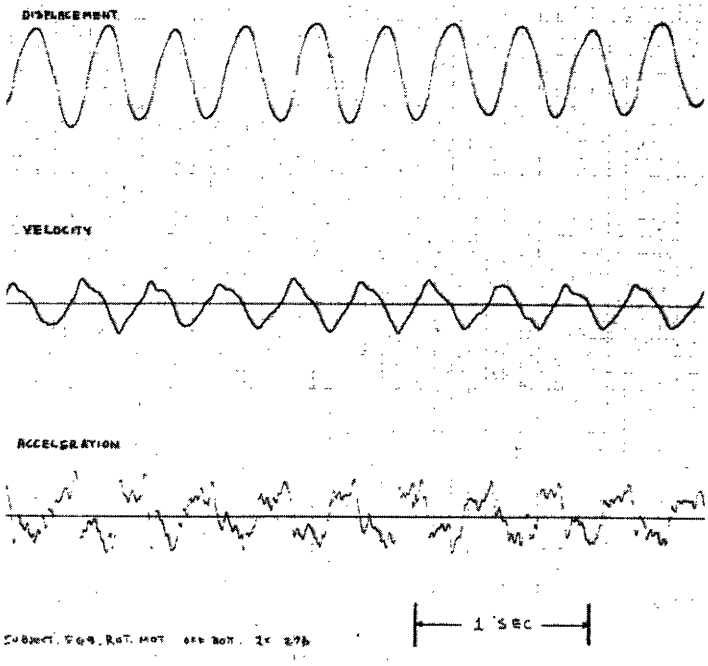

(b) PENCIL OFF BOTTOM

Fig. 10. Rotary motion – vertical projection.

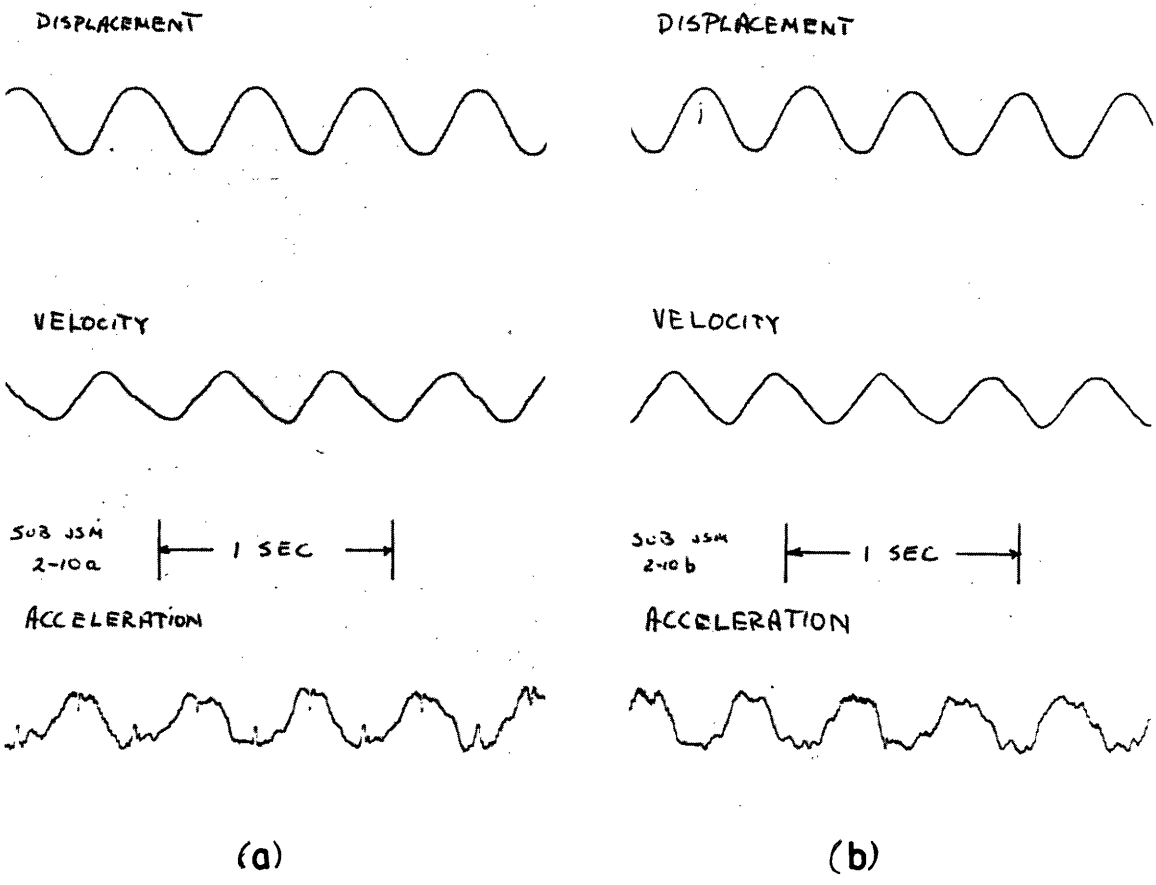

Fig. 11. Horizontal wrist motion – effect of static friction.

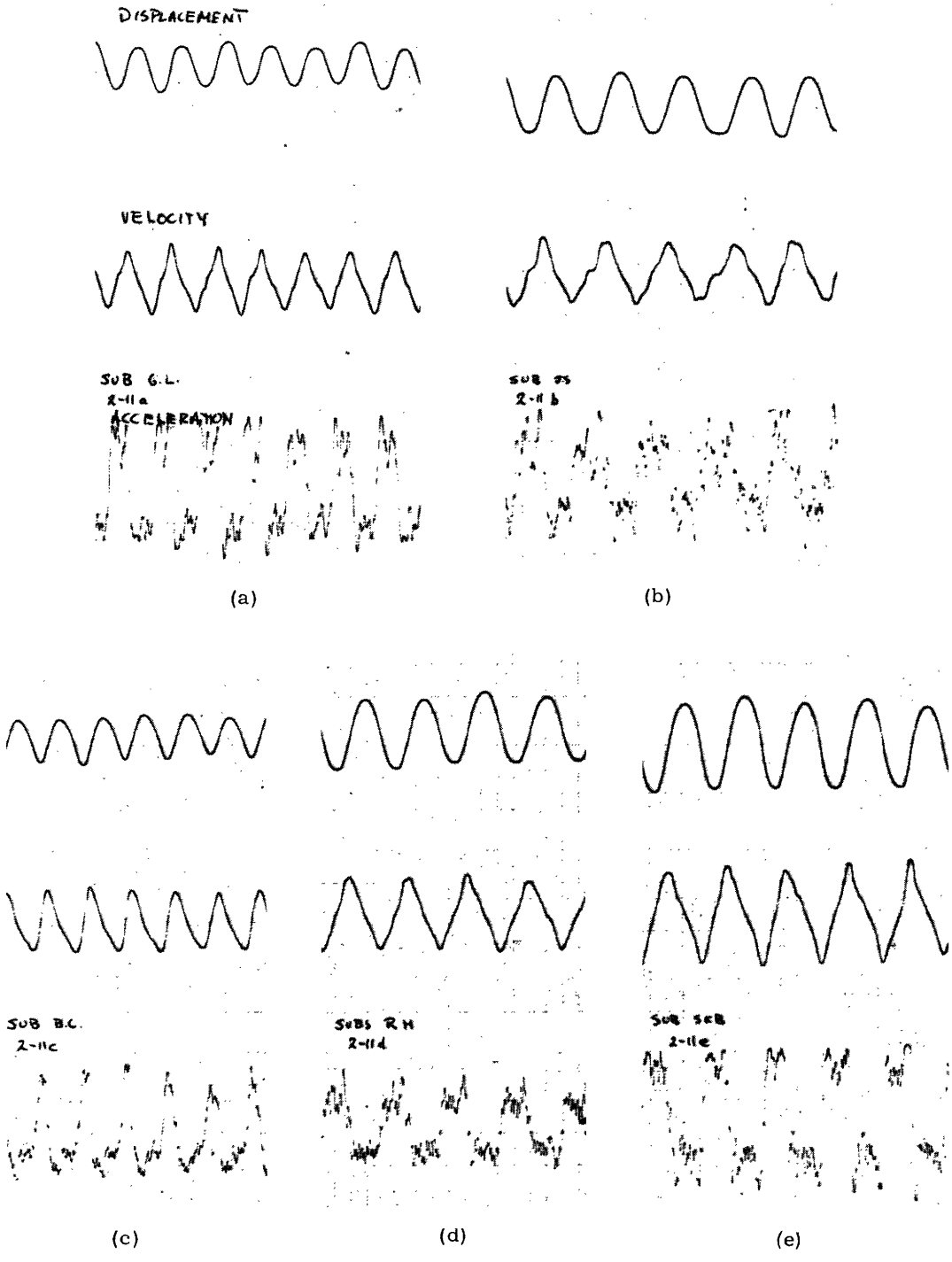

Fig. 12. Simple vertical motion – several subjects.

motion for 5 different subjects.

The acceleration waveforms appearing in Figs. 9-12 are clearly well approximated by trapezoidal waveforms. In this respect they are similar. They differ, however, in their fine structure. The fine structure can be attributed to several causes, such as relative motion of the pencil with respect to the fingers (caused by the changing of the point of contact of fingers and pencil and the spongy grip provided by the fingertips), and involuntary movements of one set of members when the primary movement is provided by another set. An example of the latter is involuntary movement of the fingers when executing left-right motions about the wrist joint. This source of fine structure is very dependent upon the posture of the hand and arm. Other sources of fine structure in the acceleration are friction between the hand and the writing surface, and tremor caused by fatigue when holding the pencil off the bottom of the tank. Interference from extraneous electrical sources appears in some of the acceleration waveforms (see, for example, the horizontal acceleration in Fig. 16b).

The various effects mentioned above have been identified by observation and experiment. In certain cases, some of the fine structure could be eliminated by clamping the pencil tightly to the finger, thereby greatly reducing the relative motion of the pencil and the hand. This effect is shown in Fig. 13 for vertical motion (Subject JSM). The amount of fine structure attributable to this source was found to vary, the amount depending on the position of the hand, the way of holding the pencil, and the individual subject involved. The order of magnitude of force represented by the changes of acceleration referred to in Fig. 13 as fine structure is not large enough to be sensed as a pressure change on the pencil grip. One can barely detect the pressure change caused by the effect of static friction, and the fine structure is less than one-third of the magnitude of the spikes resulting from static friction.

2.4 EXPERIMENTAL RECORDS – HANDWRITING

Examples of the displacement, velocity, and acceleration records of actual handwriting samples appear in Figs. 14-17. Figure 14a shows the vertical displacement, velocity, and acceleration together with horizontal acceleration, while Fig. 14b shows horizontal displacement, velocity, and acceleration, together with vertical acceleration. Figure 14c is the vertical displacement as a function of horizontal displacement. The layout of Figs. 15, 16, and 17 is the same as for Fig. 14.

The effects of static friction are in evidence throughout the records. In Fig. 14 we see an example. The arrows in Fig. 14a point to a static friction spike. In Fig. 14b the arrow on the $h'(t)$ waveform shows that the horizontal velocity is zero as expected for static friction.

The horizontal and vertical acceleration waveforms appear twice in the records associated with each sample. One pair of acceleration signals for each sample has trapezoidal approximations fitted to the waveforms. The other pair is left untouched. The reason for doing this is so that one can see the detail of actual acceleration

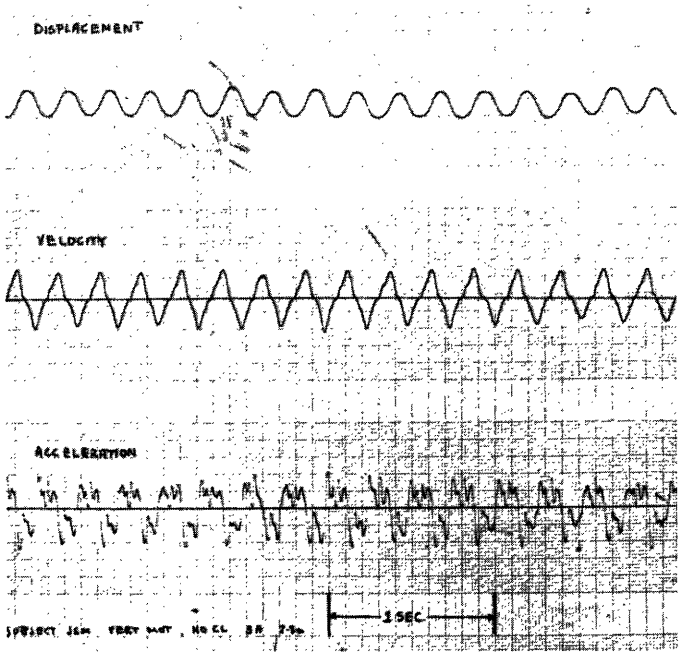

(a) CLAMP OFF

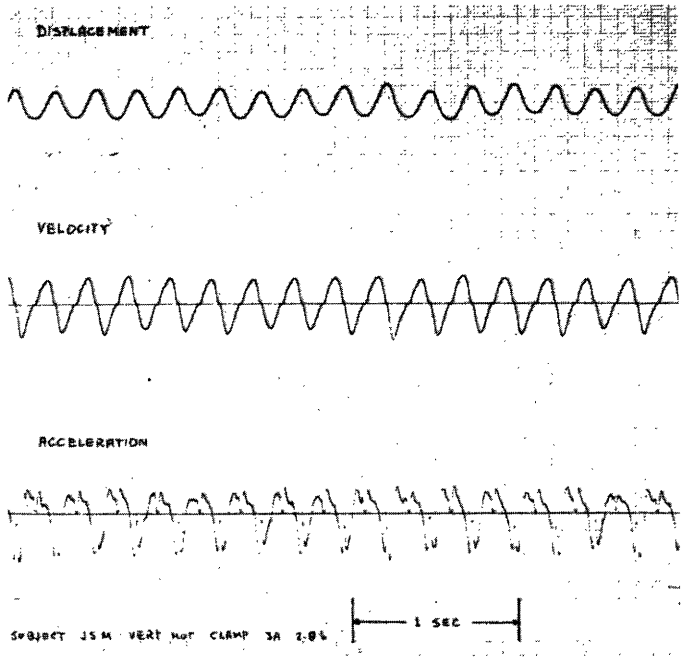

(b) CLAMP ON

Fig. 13. Vertical motion.

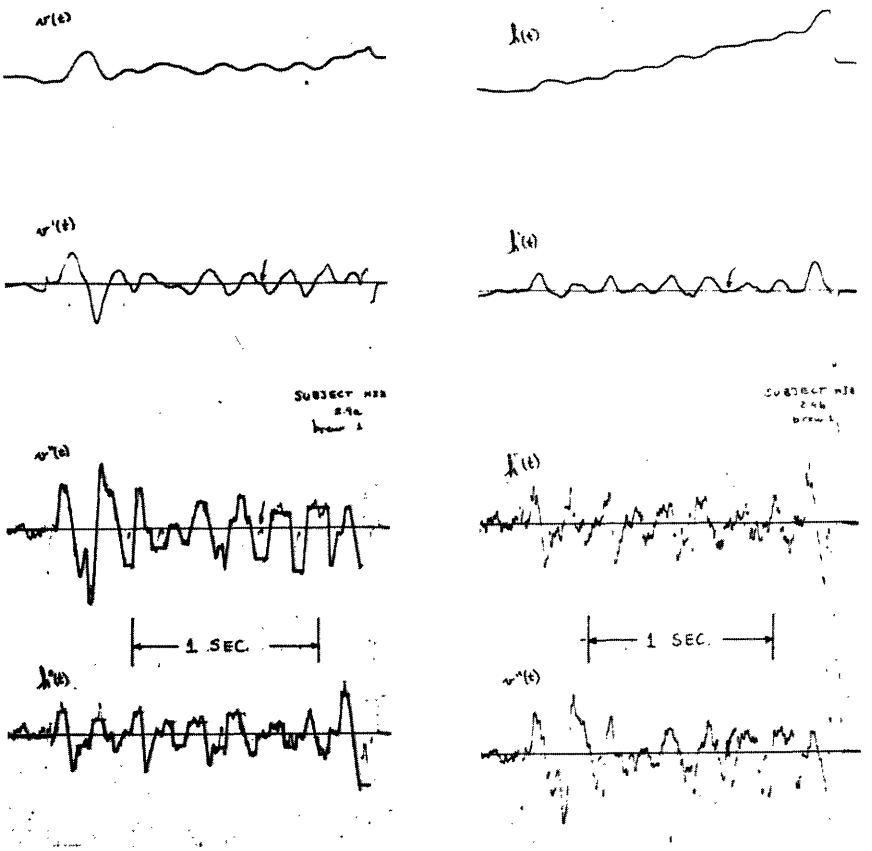

(a) (b)

(c)

Fig. 14. Handwriting sample, Subject HJZ.

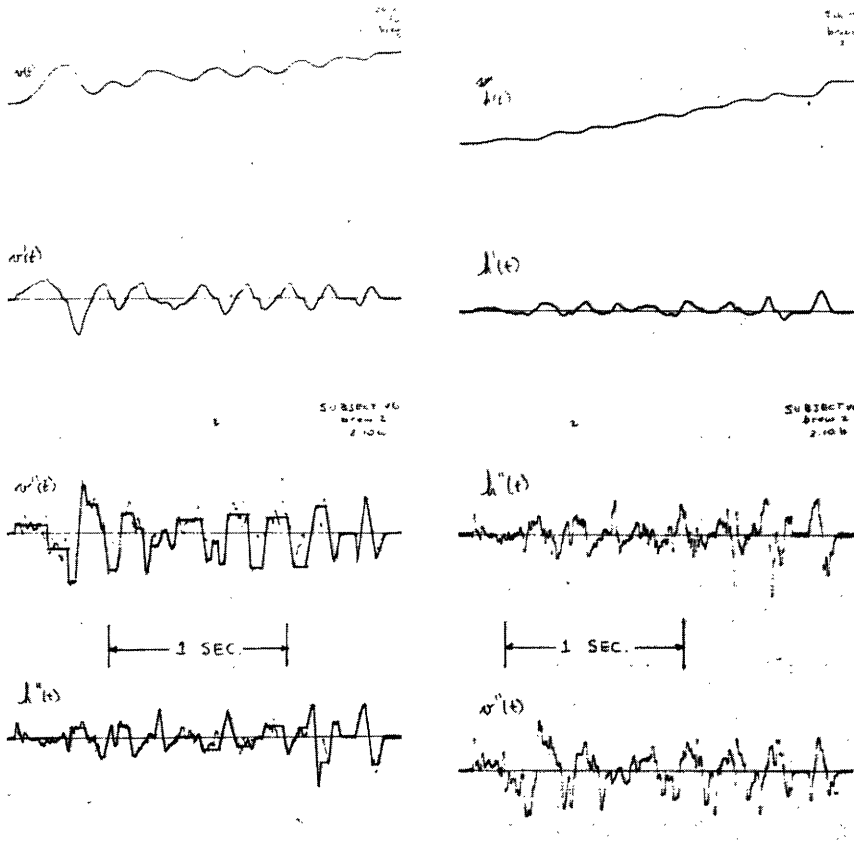

(a) (b)

(c)

Fig. 15. Handwriting sample, Subject VG.

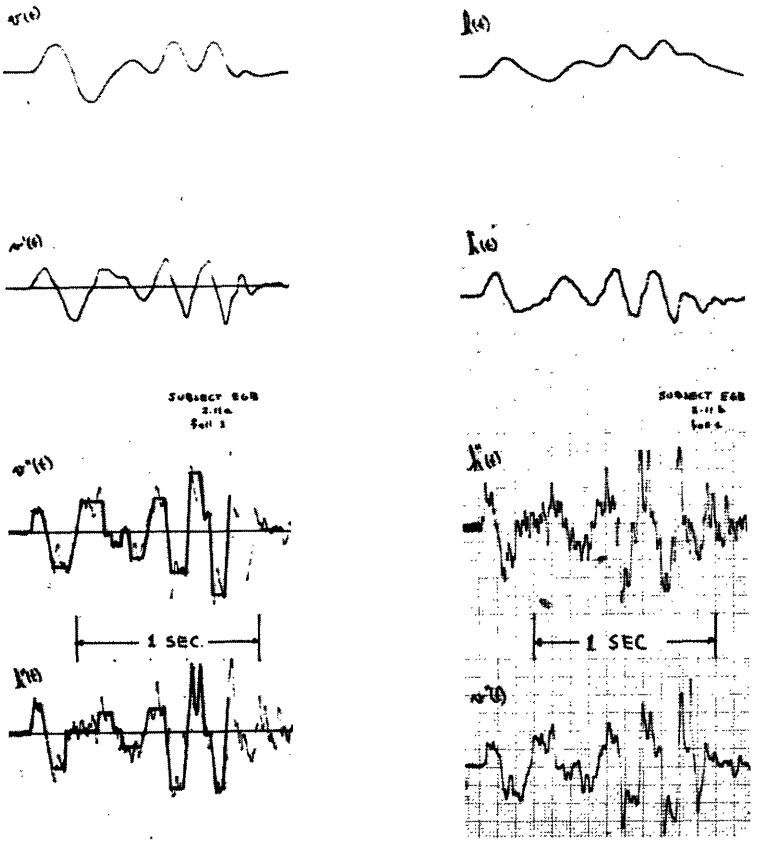

(a) (b)

(c)

Fig. 16. Handwriting sample, Subject EGB.

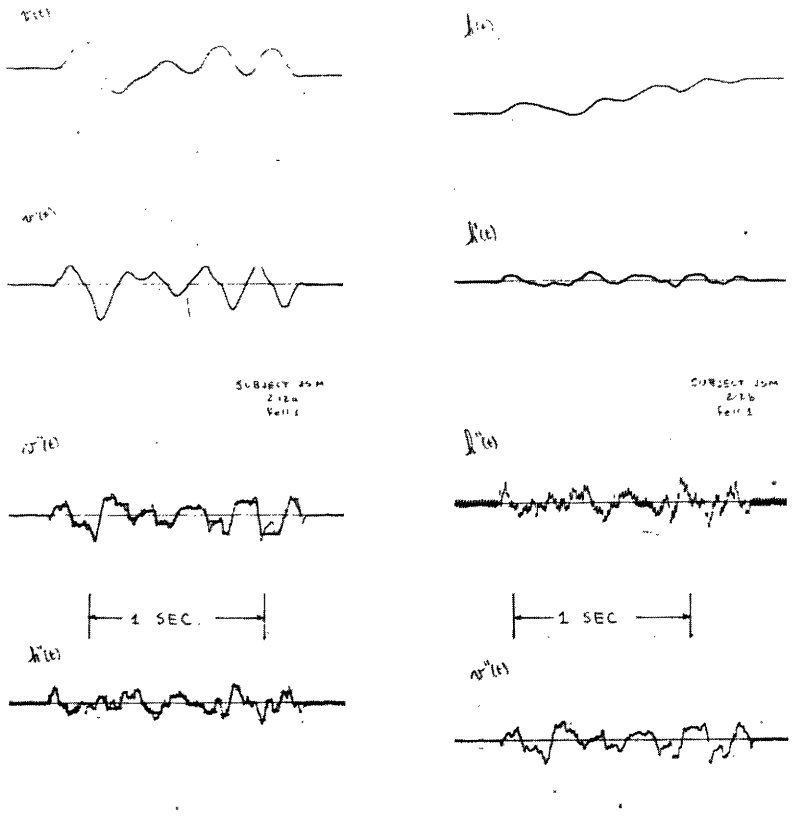

(a) (b)

(c)

Fig. 17. Handwriting sample, Subject JSM.

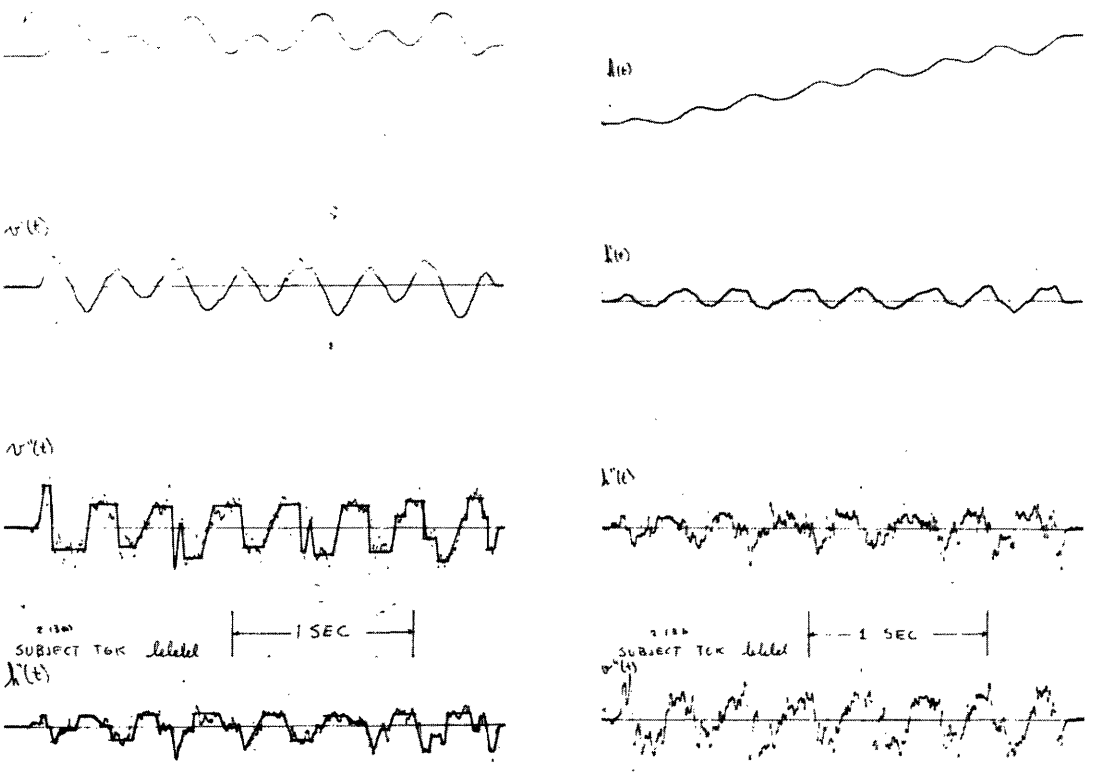

(a) (b)

(c)

Fig. 18. Handwriting sample, Subject TGK.

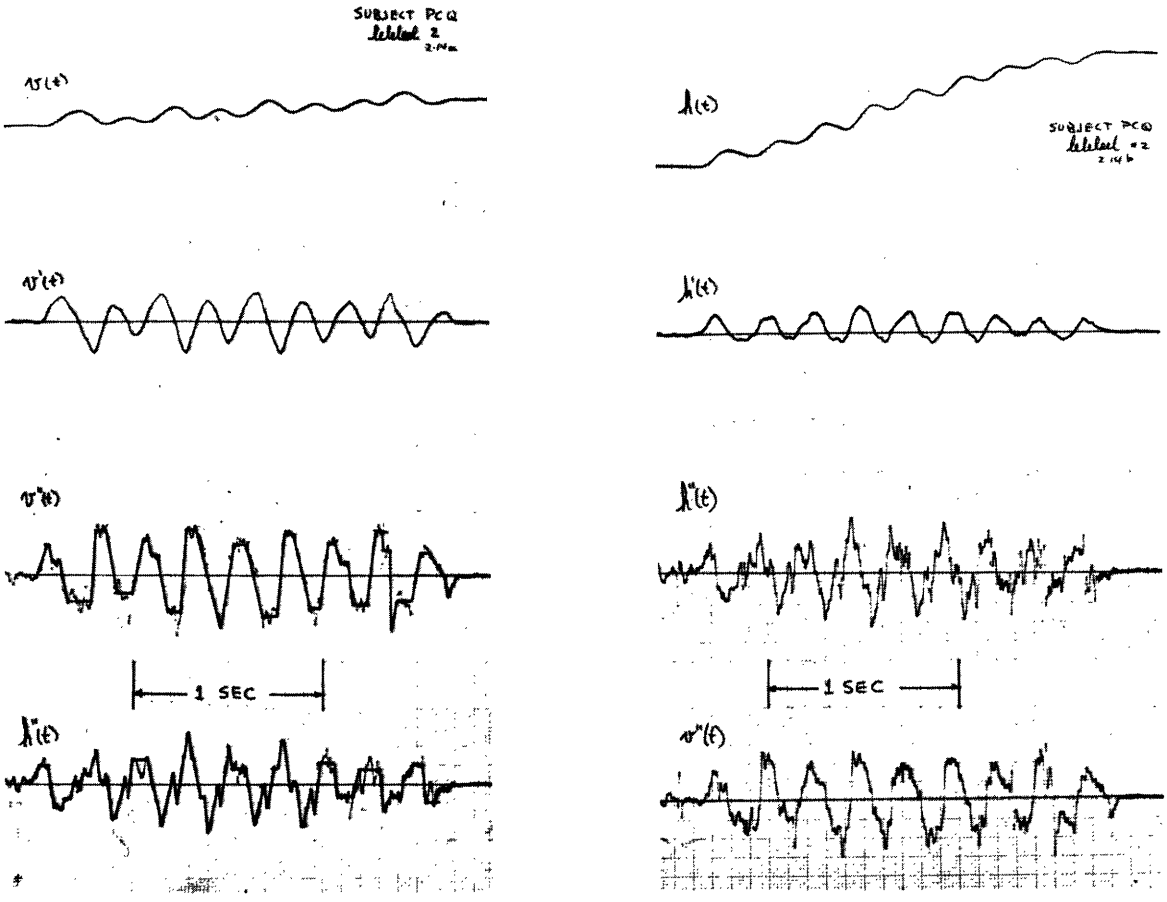

(a) (b)

(c)

Fig. 19. Handwriting sample, Subject PCQ.

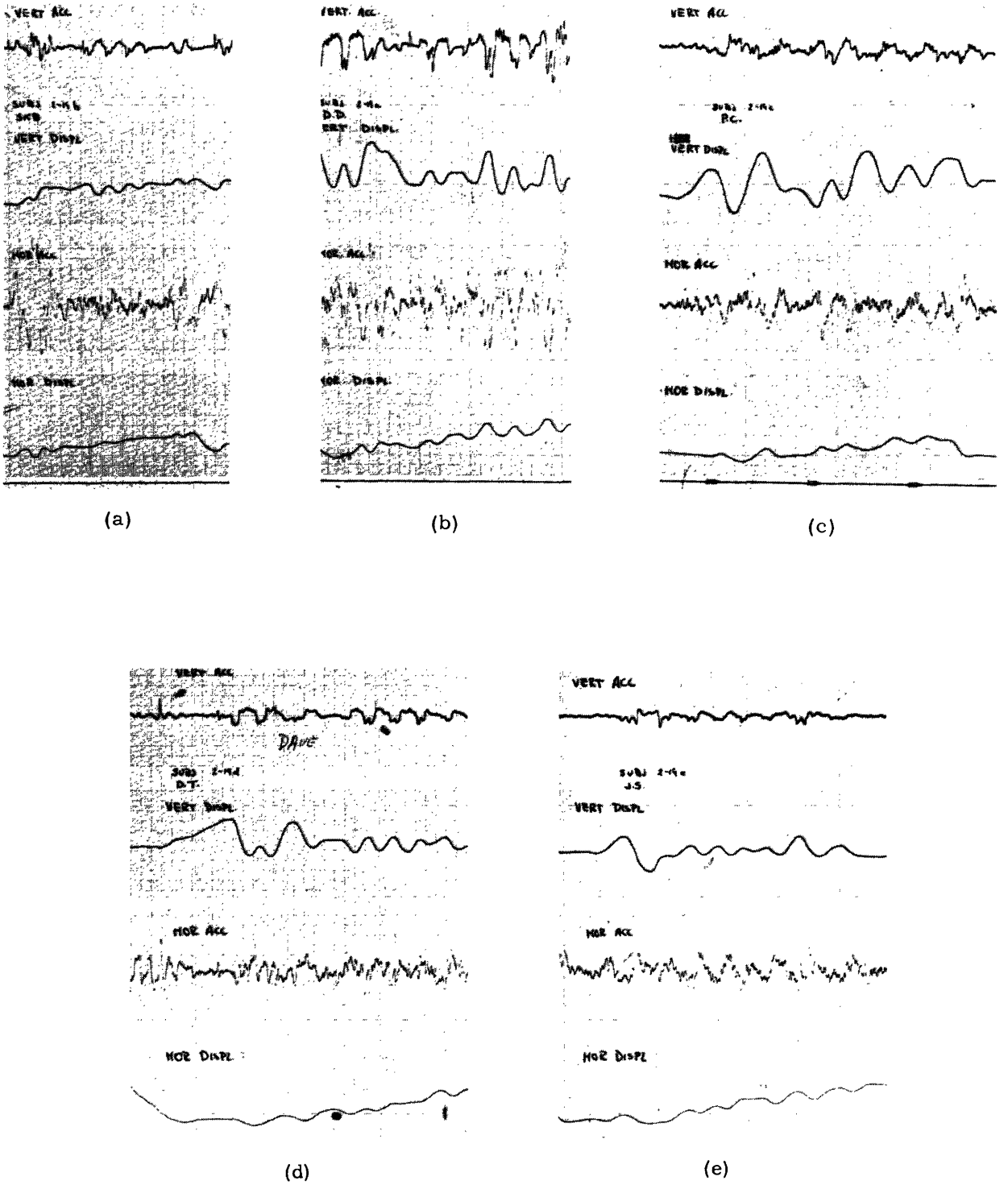

Fig. 20. Handwriting samples – five additional subjects.

waveform from which the trapezoidal approximation was made.

The technique for fitting trapezoidal approximations to the acceleration waveforms is largely intuitive, but some general guidelines can be given: Use the zero crossings as a guide to segmentation. Ignore small variations having durations of the same order as the static-function spikes. Ignore static friction effects. It is often helpful to refer to the velocity waveform when constructing a trapezoidal approximation to the acceleration waveform.

The next three figures, Figs. 18, 19, and 20, are further illustrations of the trapezoidal approximation to the acceleration of handwriting movements.

2.5 EXPERIMENTAL RECORDS – SPEED OF MOVEMENT

This section is concerned with the various aspects of slow and fast hand movement. Specifically, we shall consider a simple left-right motion of the hand about the wrist joint as the frequency of the movement is increased. This movement was chosen as an example because it is easy to control and is a simple basic movement. Figure 21a, 21b, and 21c displays various sections of a continuous record of movement with steadily increasing speed. The entire record was taken with the pencil lifted to eliminate the effects of static friction. Figure 21a and 21b shows the displacement velocity and acceleration of wrist movement for relatively slow movement. Notice that the acceleration is very "pulselike," and the control is apparently discontinuous. In fact, the acceleration waveforms in these two records are quite amenable to trapezoidal approximation, although each section of the trapezoid is very short and contributes very little to the displacement as contrasted to those trapezoidal sections shown previously. Figure 21b shows the beginning of the trend of the small trapezoidal segments of the acceleration waveform to form a larger trapezoidal pattern, in that they are alternately predominant above and below the zero axis. Figure 21c shows the transition to this situation in the place near the end of this record where the fine structure in the acceleration waveform alternates above and below the axis, giving the over-all appearance of a large trapezoidal wave. As the speed of movement continues to increase, there is a quite sudden transition to a "clean" trapezoidal wave. This transition is shown in Fig. 21d where the acceleration waveform toward the end of this record is of the nature of those found in handwriting. Figure 21e shows the transition from conventional trapezoidal form to a more triangular-shaped waveform as the frequency of the movement reaches its highest value. The frequency at this point is approximately 4 cycles, and although one can go a cycle or two faster than this, there is no change in the basic shape of the waveforms beyond this point. Movements of the type depicted in Fig. 21a through 21c will be referred to as "continuously controlled movements," while those in Fig. 21d and 21e will be called "stroke-controlled" movements. The inference here is that slower movements are controlled in semicontinous fashion (as in a sampled-data system), whereas fast movements are controlled on a stroke-by-stroke basis.

Examples of both types of control of movement sometimes occur in the same

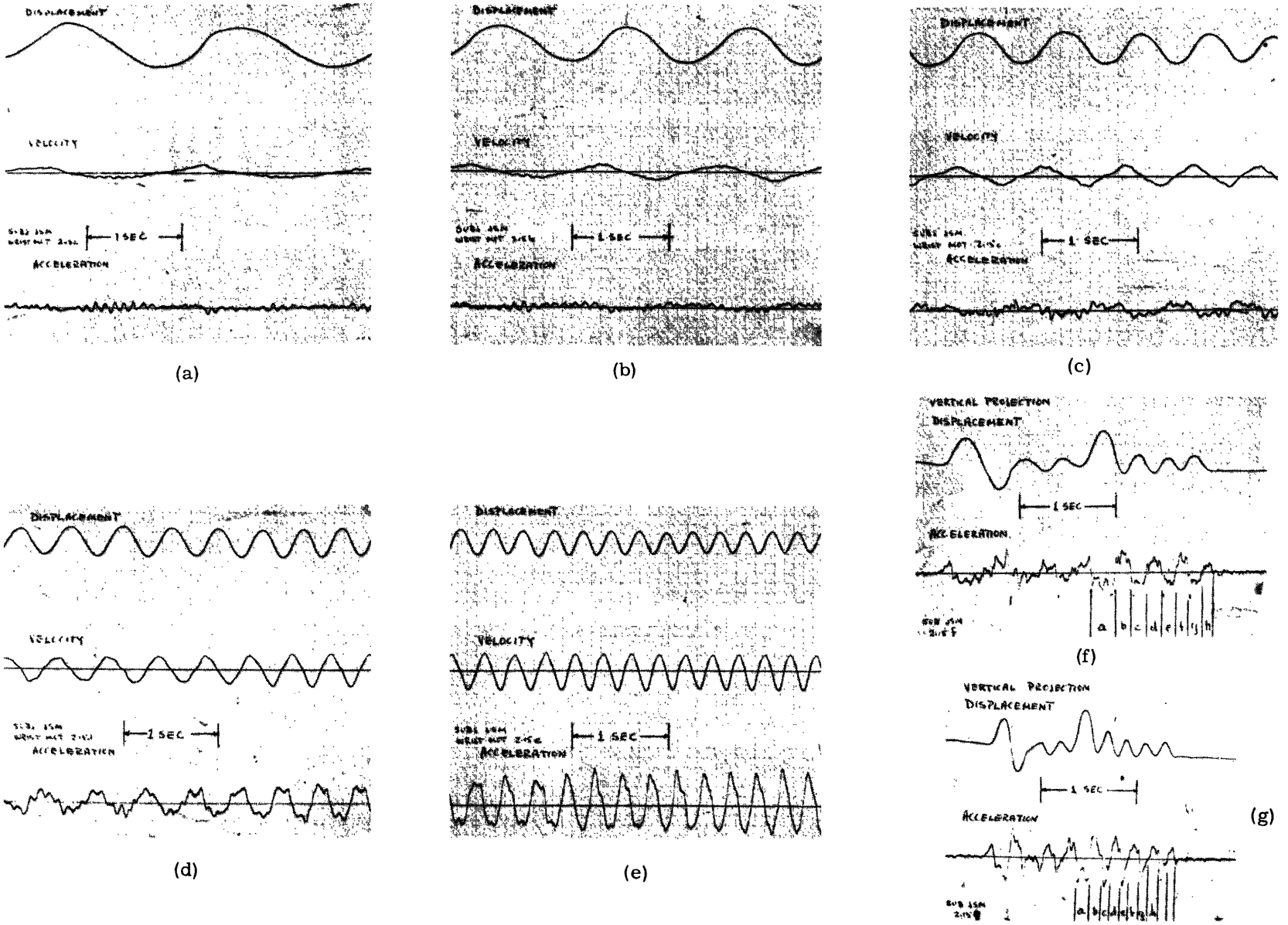

Fig. 21. Waveforms for various speeds of movement.

handwriting sample. Such a sample appears in Fig. 21f. Here the subject tried to write "John" as slowly as possible. The vertical projections of displacement and acceleration are shown. Continuous control is in evidence in the first part of the sample, while the last part is stroke-controlled. Section "a" of the stroke-controlled portion represents the transition from one type of control to the other (as in Fig. 21d, as the speed of the writing increased slightly throughout the execution of the sample). Figure 21g shows the same word written as fast as possible by the same person. The last part of the word is segmented to correspond to the segmentation of the stroke-controlled portion of Fig. 21f. The two extra segments occur because the last letter turned out to be an "m" instead of an "n", but that is what happens when you hurry. Both of these records were taken at the same time with the pencil lifted to reduce the effects of friction.

The records presented in Fig. 21 show that the acceleration of carefully controlled movements can be approximated by trapezoidal waveforms independently of the speed of the movement, but there are two distinct types of control of that movement; that which we have called "continuous" and that which we have called "stroke." Furthermore, there is a fairly abrupt transition between the two types of control, which depends on the speed of the movement. This fact indicates that the nervous processes controlling slow and fast movements may be quite different.

2.6 ACCELERATION RISE TIMES FOR VARIOUS MOVING MEMBERS IN A SINGLE SUBJECT

A close correlation has been observed between the size of the member (and hence the musculature) that is being moved in a particular motion and the rise time of the trapezoidal acceleration waveform.

Figure 22 illustrates this very well. The four sets of waveforms shown there were made by the movement of certain specific parts of the anatomy. Figure 22a is to-and-fro motion of the fingers holding a pencil. Figure 22b is a record of motion of the fingers from left to right while holding a pencil. In Fig. 22c, motion is about the wrist joint. That is, with the fingers held rigid, the hand is swung from left to right. Figure 22d shows waveforms obtained when the entire arm is moved to and fro (i.e., rotation about the shoulder joint).

The rise time of the acceleration waveforms is seen to increase with increasing size of the moving member. The rise time of the acceleration in Fig. 22d, which arises from the large muscles acting upon the shoulder joint, is approximately 1/10 of a second. This rise time is so long that for the repetition rate of the movement shown, the trapezoidal wave degenerates into a triangular wave.

2.7 COMMENTS ON EXPERIMENTAL RECORDS

The results displayed in Figs. 9 through 20 are typical examples taken from a large number of samples. In all, 14 people are responsible for the samples of simple motions and handwriting presented here. Each of the 11 samples of handwriting in Figs. 14

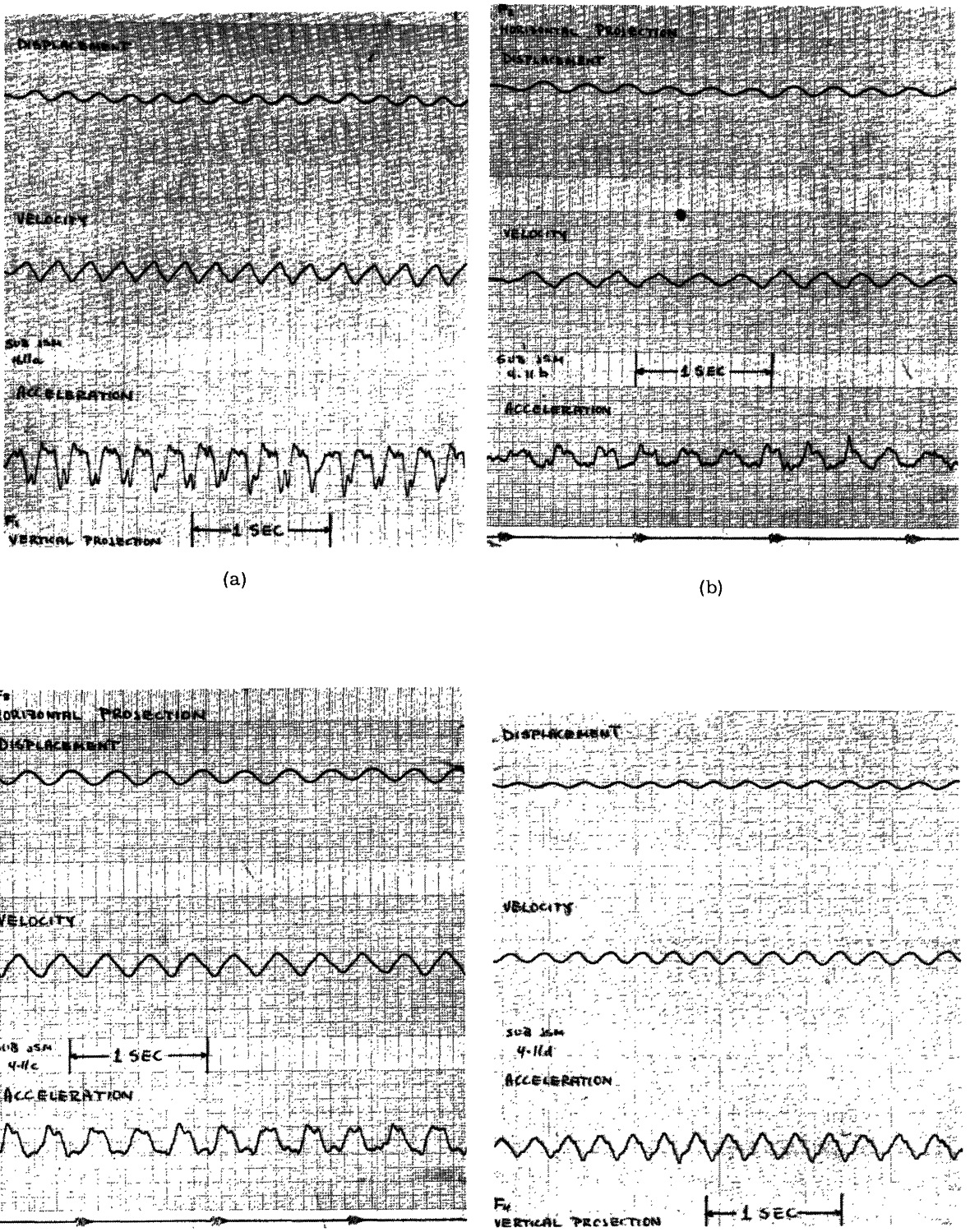

Fig. 22. Waveforms for action of different muscle groups.

through 20 is from a different person.

The dominant aspect of the acceleration waveforms in these records is the zero crossings, which indicate a significant change in applied force. Figure 23a shows a typical acceleration waveform. The zero crossings referred to are marked "x". Figure 23b shows the same waveform with a trapezoidal approximation. The considerable irregularity of the "flat" part of the acceleration waveform has been ignored in making the trapezoidal approximation. How much of this fine structure, if any, is attributable to the function of the biological system and how much is due to friction and other mechanical phenomena is a question that cannot be answered here. In making a trapezoidal approximation, we are assuming that the fine structure is not important to handwriting, and all that really matters are the large abrupt changes in the acceleration. The simulations to be presented in Section III support this assumption.

Concerning the possible effect of dry sliding friction: If sliding friction is significant, then the portion of the acceleration waveform following a static-friction spike should be lower in absolute value than the part preceding the spike, since the direction

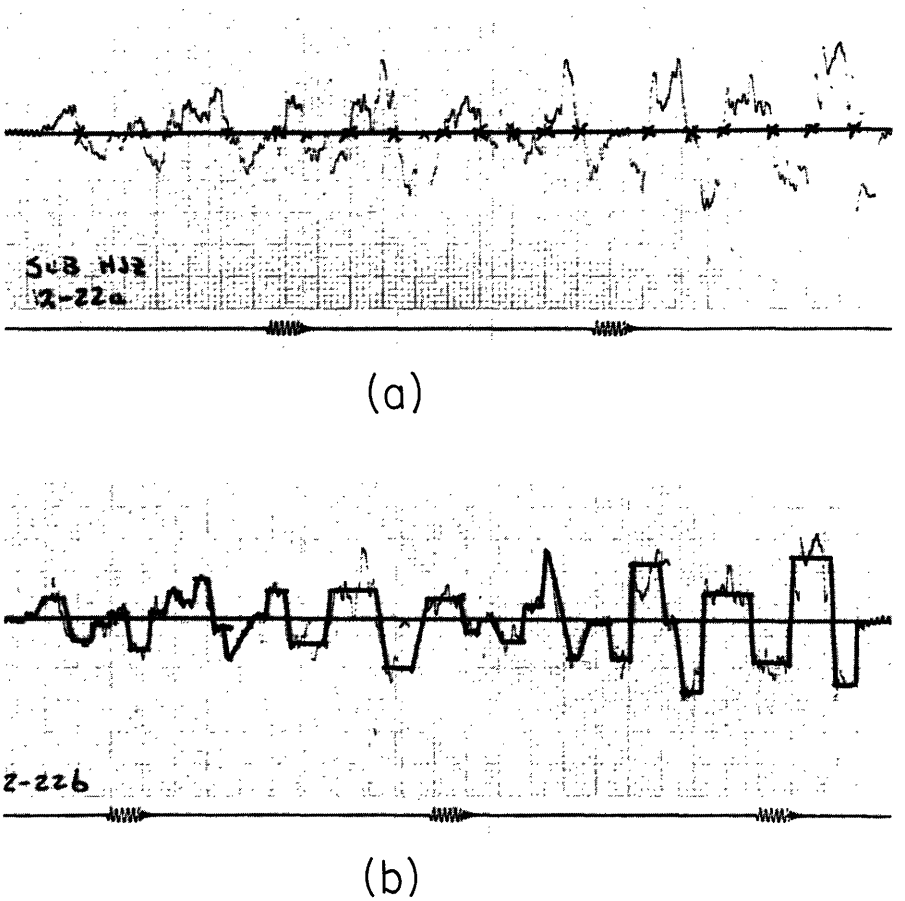

Fig. 23. Typical acceleration waveform.

of velocity is reversed and sliding friction is opposing the motion. Of 109 occurrences of static friction spikes in 30 samples of handwriting, only 49 were found to exhibit the above-mentioned behavior. We thus conclude that either sliding friction is not significant or the human system somehow compensates for it immediately.

The results presented in section 2.4 also show that the acceleration signals have more than two levels. If we allow that the two independent directions assumed by Denier van der Gon[1] are not the ones that we have chosen to record, then we would get a maximum of 4 levels in any direction. This is illustrated in Fig. 24, where two non-orthogonal independent directions have been chosen and two arbitrary levels set off in each direction. It is easily seen from the figure that there are at most 4 levels projected onto each of the horizontal and vertical axes.

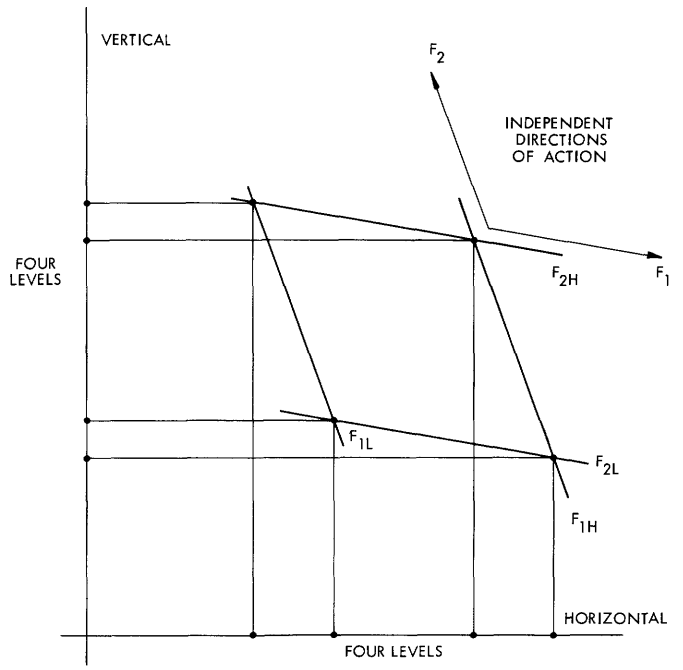

Fig. 24. Projections of two-level forces.

Inspection of Figs. 14-17 reveals that in general there are more than 4 levels in each of the acceleration waveforms. Even in Fig. 19, which is a sample of lelele, we find more than 4 levels in the acceleration waveforms. Figure 18 is a fairly uniform sample of lelele, and it comes closer to satisfying the two-level assumption. Thus we see that some samples of lelele do have nearly the same force on all segments of the trapezoidal wave, but this is a particular case rather than a general truth for handwriting.

III. A SYSTEM THAT SIMULATES HANDWRITING

3.1 INTRODUCTION

The handwriting samples and associated waveforms presented in Section II have shown that one should be able to simulate handwriting quite closely by using a modification of the basic scheme proposed by Denier van der Gon, Thuring, and Strackee[1]; namely, a simulation of a point mass with viscous friction driven by a force waveform that is a trapezoidal time function having more than two levels. The differential equation for the assumed system is

$$m\frac{d^2x}{dt^2} + k\frac{dx}{dt} = f(t), \tag{1}$$

where m is the mass, k is the viscous friction coefficient, x is the displacement, and f is the applied force.

Consider first the solution of Eq. 1 when f(t) is a step function $f(t) = Fu_{-1}(t)$ with $\frac{dx}{dt}(0) = v_o$, $x(0) = 0$. This solution is

$$x(t) = \frac{F}{k}t + \frac{m}{k}\left(v_o - \frac{F}{k}\right)\left(1 - e^{-\frac{k}{m}t}\right) \qquad t \geq 0$$

$$x'(t) = \frac{F}{k} + \left(v_o - \frac{F}{k}\right)e^{-\frac{k}{m}t} \qquad t \geq 0$$

$$x''(t) = -\frac{k}{m}\left(v_o - \frac{F}{k}\right)e^{-\frac{k}{m}t} \qquad t \geq 0 \tag{2}$$

For the special case k = 0, we get

$$x(t) = \frac{F}{2m}t^2 + v_o t \qquad t \geq 0$$

$$x'(t) = \frac{F}{m}t + v_o \qquad t \geq 0$$

$$x''(t) = \frac{F}{m} \qquad t \geq 0 \tag{3}$$

The response of the same system to a ramp function input $f(t) = Ru_{-2}(t)$ is

$$x(t) = \frac{R}{2k}t^2 + \frac{m}{k}\left(v_o - \frac{R}{k}\right)\left[t - \frac{m}{k}\left(1 - e^{-\frac{k}{m}t}\right)\right] \qquad t \geq 0$$

$$x'(t) = \frac{R}{k}t + \frac{m}{k}\left(v_o - \frac{R}{k}\right)\left(1 - e^{-\frac{k}{m}t}\right) \qquad t \geq 0$$

$$x''(t) = \frac{R}{k} + \left(v_o - \frac{R}{k}\right)e^{-\frac{k}{m}t} \qquad t \geq 0 \tag{4}$$

For the special case k = 0, we get

$$x(t) = \frac{R}{6m} t^3 + \frac{v_o}{2} t^2 \qquad t \geq 0$$

$$x'(t) = \frac{R}{2m} t^2 + v_o \qquad t \geq 0$$

$$x''(t) = \frac{R}{m} t \qquad t \geq 0 \tag{5}$$

The response of the system to a trapezoidal input f(t) is easily constructed from Eqs. 2 and 4. Figure 25 is a plot of a typical solution.

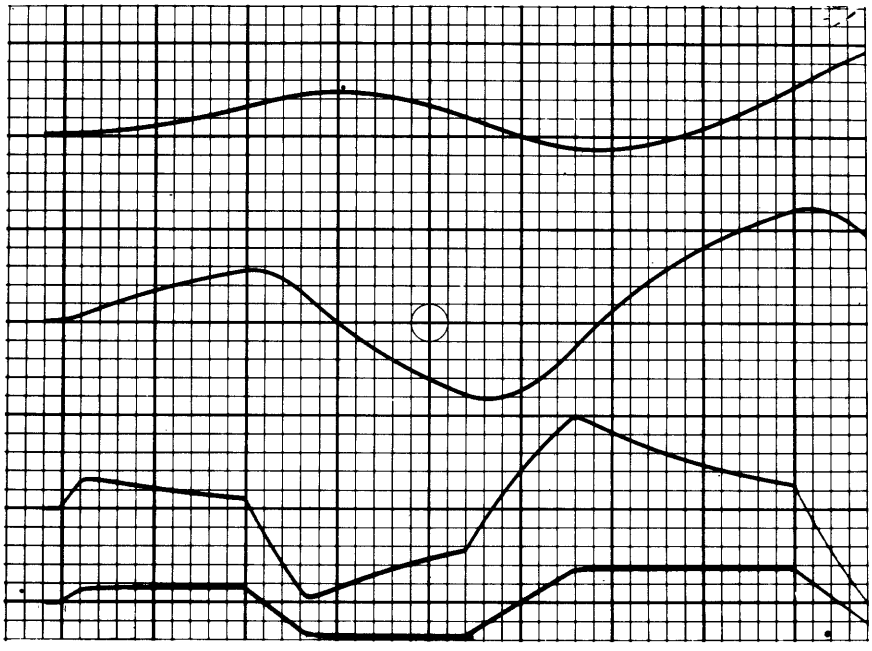

Fig. 25. Solution of Eq. 1 for trapezoidal f(t).

A physical question arises concerning the inclusion of the effect of friction in the system. The records in Section II show the effect of static friction quite plainly, but we have chosen to ignore it. Dry sliding friction was discussed in section 2.7 and found to be negligible. Neglecting the effect of static friction, one is left with an uncertainty of approximately 25% of the mean height for the trapezoidal wave's flat top in the experimental records. There is no definite trend in the droop of the trapezoidal wave, so this gives us a bound on the droop of ~25% over the duration of the longest segment. Let T be the duration of the longest segment of the trapezoidal wave in seconds, then for 25% droop, $e^{-\frac{k}{m}T} = 0.75$, and $\frac{k}{m} T = 0.29$ or $\frac{k}{m} = \frac{0.29}{T}$. This gives an upper bound on $\frac{k}{m}$ in terms of T:

$$\frac{k}{m} \leq \frac{0.29}{T} . \tag{6}$$

Typically, T = 0.12 sec, so this gives $\frac{k}{m} \leq 2.42$. This figure is only a rough upper bound, and the ratio $\frac{k}{m}$ may, in fact, be much lower.

An electronic simulator has been constructed which mechanizes Eq. 1 where the trapezoidal wave f(t) is allowed to take on a continuum of amplitude values. This simulator, its adjustment, and some of the experiments in which it has been employed are the subjects of this part of the report.

3.2 THE SIMULATOR

A functional block diagram of the handwriting simulator appears in Fig. 26. The simulator consists of two principle parts: the linear system which simulates Eq. 1 and provides for independent adjustment of m and k, and the trapezoidal wave generator which provides the "force" signal f(t). The use of an oscilloscope for displaying the

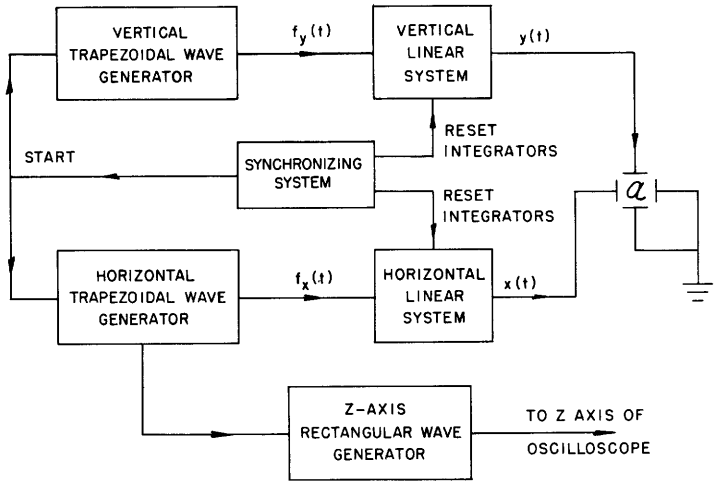

Fig. 26. A handwriting simulator.

output of the system requires two linear systems and two trapezoidal-wave generators, one for vertical deflection and one for horizontal deflection. A synchronizing system provides the start pulse for the trapezoidal-wave generators, and the reset signals to discharge the integration capacitors in the linear system.

Operation of the simulator is as follows: The synchronizing system contains an oscillator that generates integrator reset signals at a frequency that can be set by a front-panel control. The integrator reset signal is of 5 msec duration (reset interval or clamp period). The start pulse for the trapezoidal-wave generators occurs at the end of the reset interval (see timing diagram, Fig. 27). This start pulse initiates a burst of trapezoidal waves from each trapezoidal-wave generator. Each segment of the trapezoidal wave can be varied by two controls in the generator; one control adjusts

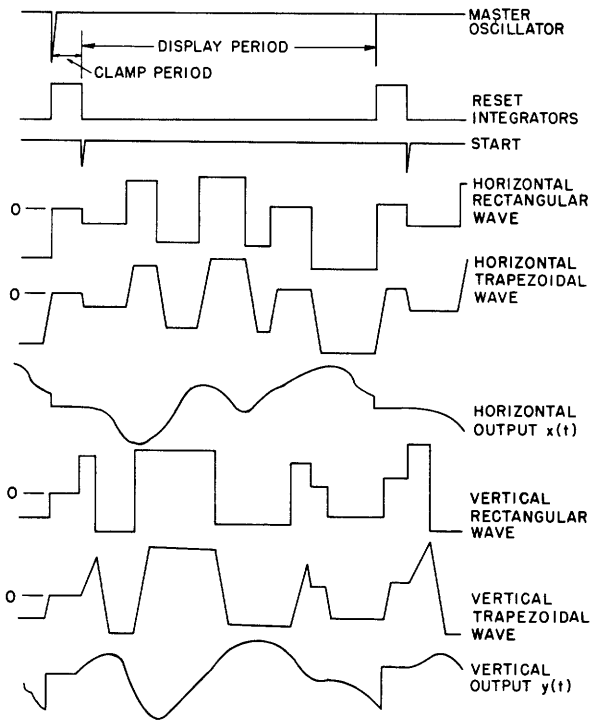

Fig. 27. Timing diagram for the simulator.

the amplitude of the segment, and the other adjusts its duration. Switches are provided to switch the segments of the trapezoidal wave on in sequence. As more segments are added to the trapezoidal wave during the setup procedure, the frequency of the oscillator in the synchronizing system must be decreased to avoid overlapping of successive trapezoidal wave trains.

A rectangular wave generator[13] is provided to blank the z-axis of the display oscilloscope to simulate lifting of the pencil during the writing movement. This generator can receive its input triggers from any point in either the horizontal or vertical trapezoidal-wave generators or both. In Fig. 26 it is shown receiving input from the horizontal generator.

3.3 OPERATION OF THE SIMULATOR

Figure 28 illustrates the operation of the simulator. The three sections of this figure show various stages in setting up simulation of the word "brew." In Fig. 28a, the b is almost complete. The waveforms in the lower half of the picture are from top to bottom: vertical displacement (y(t)), vertical trapezoidal wave ($f_y(t)$), horizontal displacement (x(t)), horizontal trapezoidal wave ($f_x(t)$). In tracing this much of the sample, the repetition rate of the oscillator is such that three repetitions of the time waveforms appear in the picture. As the simulation progresses, more sections are added to the trapezoidal wave, and the oscillator frequency is reduced to allow the additional sections to be fitted in. As each segment of the trapezoidal wave is added,

(a)

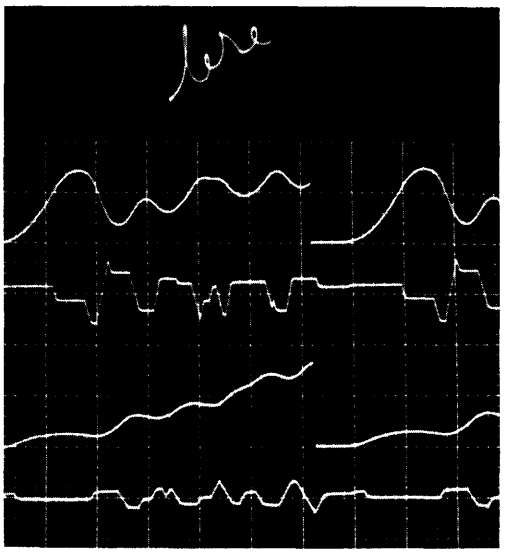

(b)

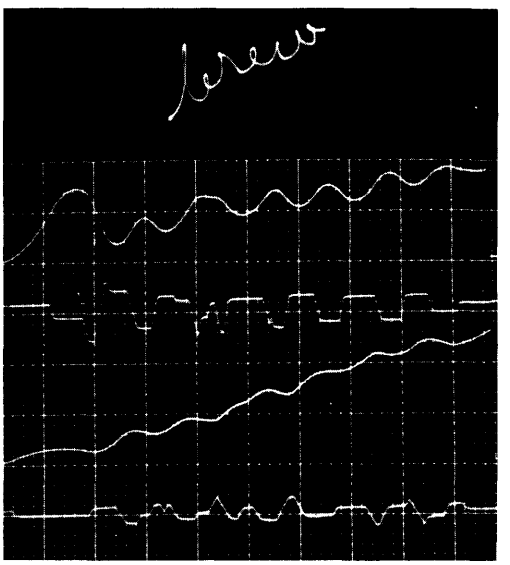

(c)

Fig. 28. Setting up the simulator.

it is adjusted in both duration and amplitude to make the resulting output correspond as closely as possible to the pattern that is being copied. Figure 28b shows completion of "bre", and Fig. 28c shows the completed simulation. The time and amplitude scale factors in all three pictures in Fig. 28 are identical.

When copying a specific sample of handwriting, the sample is recorded on transparency film or thin paper, and is inserted into the projected graticule attachment on a Tektronix C-12 oscilloscope camera. A ground glass on the back of the camera then has the image of the sample superimposed upon the image of the trace on the oscilloscope. The simulator is adjusted to make the two images coincide.

3.4 SIMULATION OF HANDWRITING

Figures 29-32 display the results of simulating the four samples displayed in Figs. 13-17. In each of these, the trapezoidal waveforms were set up to match as closely as possible with the trapezoidal approximation to the actual acceleration. The trapezoidal waves were then trimmed to give close match between the output and the original sample.

The leading and trailing slopes of the trapezoidal waves are independently adjustable, but there is no independent adjustment for each segment of the wave. Inspection of the records presented in Section II clearly reveals that the slopes on the various segments of the trapezoidal waves are not the same. This, together with the fact that the effect of static friction is neglected, accounts for the most noticeable discrepancies between the original and simulated handwriting.

Figure 29 is a simulation of the word "brew" displayed in Fig. 14. In Fig. 29a, the top word is the simulation, the bottom one is the original word as written by the subject. Figure 29b shows waveforms taken from the simulator which correspond to those of Fig. 14a. The effect of the uniform leading slope required by the simulator can be seen as a more rounded tip on the first negative peak in the vertical velocity waveform $v'(t)$ in Fig. 29b than appears on the same waveform in Fig. 14a. This occurs because the slope on the vertical acceleration waveform is too low at this point. On the other hand, the fifth positive segment of the vertical acceleration waveform of Fig. 29b is wider than it should be because the slope at this point is too large compared with the actual waveform of Fig. 14a. Figure 29c shows the set of simulator waveforms corresponding to Fig. 14b.

Using Figs. 14 and 29, together with the settings of the linear system in the simulator, we compute an equivalent value of $\frac{k}{m}$ for the simulation of Fig. 29 to be

$$\frac{k}{m} = 2.88.$$

From Fig. 15, the duration of the longest segment ≈ 0.13 second. Hence, according to Eq. 6,

$$\frac{k}{m} \leq \frac{0.29}{0.13} = 2.2.$$

(a)

(b)

HORIZONTAL SCALE

5 ms/large division

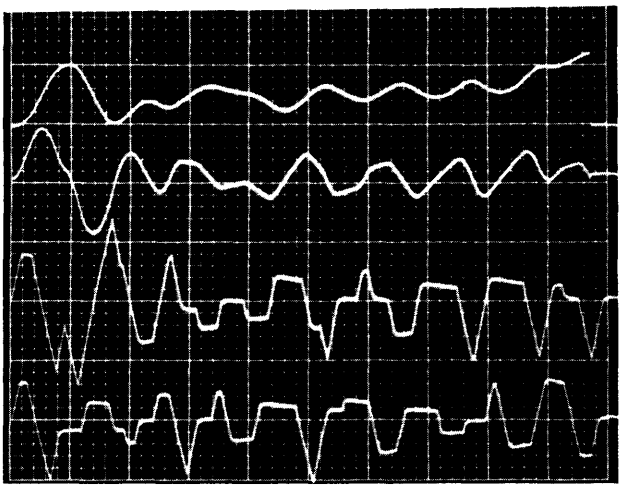

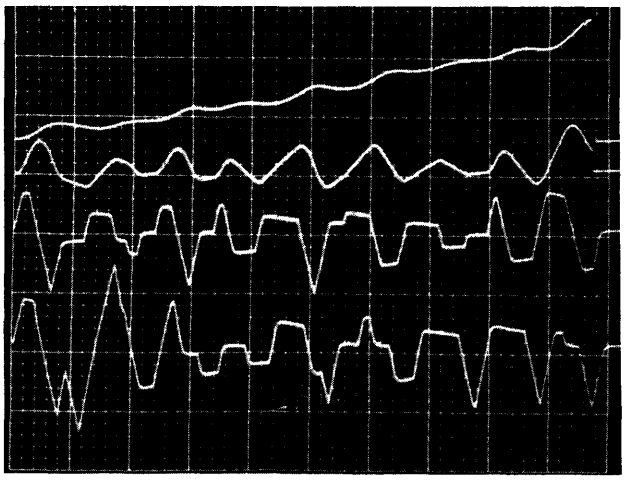

(c)

Fig. 29. Simulation of sample of Fig. 14.

(a)

(b)

HORIZONTAL SCALE

5 ms / large division

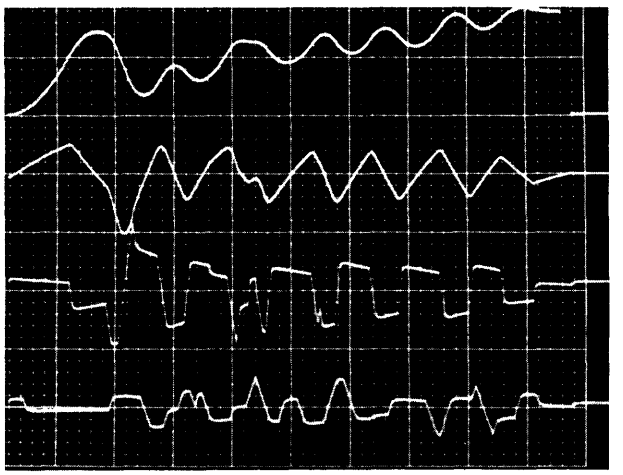

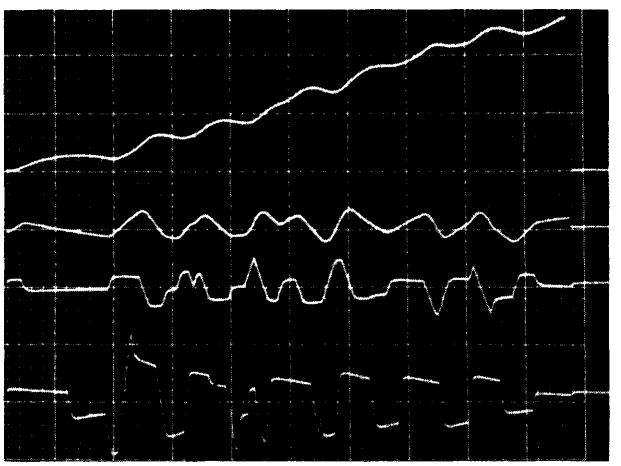

(c)

Fig. 30. Simulation of sample of Fig. 15.

(a)

(b)

HORIZONTAL SCALE

5 ms/large division

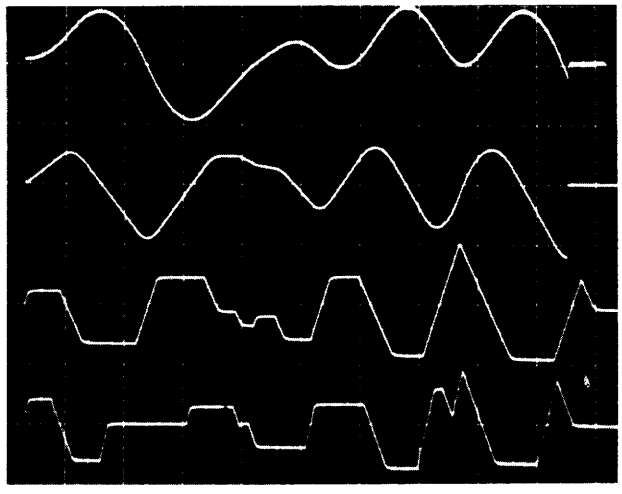

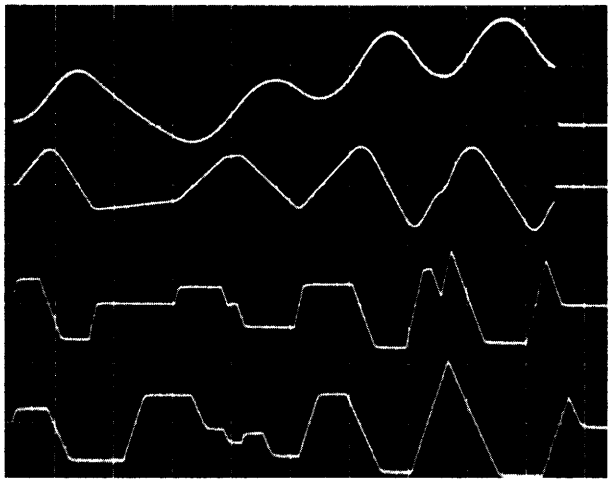

(c)

Fig. 31. Simulation of sample of Fig. 16.

(a)

(b)

HORIZONTAL SCALE
6 ms/large division

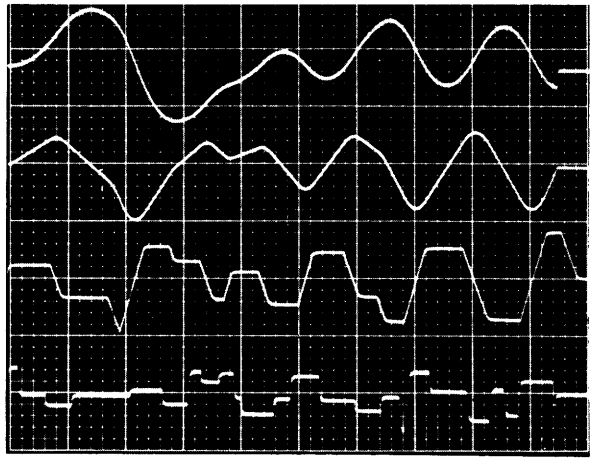

(c)

Fig. 32. Simulation of sample of Fig. 17.

Thus the friction in the simulation of this example is slightly exaggerated. The droop on the acceleration waveforms of Fig. 29 is still not too pronounced, and there is no noticeable sag on the rises of the trapezoidal wave. It is clear that one could fit a waveform having about this much droop to the acceleration waveforms of Fig. 14a just as well as the one having no droop which has been fitted in this figure. The conclusion is then that all we can say regarding the characteristics of the linear system in the model is that $\frac{k}{m}$ has an upper bound of $\frac{0.29}{T}$, where T is the duration of the longest segment.

It has been observed that the value of $\frac{k}{m}$ does not seem to affect one's ability to simulate a given sample. Figure 30 is a simulation of the word "brew" by a second subject, and it corresponds to Fig. 15. The linear system settings for this simulation are the same as the ones used in the example of Fig. 29. In Figs. 31 and 32, we have simulations of the word "fell" written by two different subjects, which correspond to Figs. 16 and 17, respectively. The value of $\frac{k}{m}$ set on the linear system for these simulations was zero! The layout of the figures and the comments that one can make about them are the same as for Fig. 29.

The four samples shown in Figs. 14-17 are written by four different people. It is particularly interesting to consider the physical characteristics of the subjects writing "fell" in Figs. 16 and 17. One of these is a tall man with large hands, while the other is a shorter man with significantly smaller hands. The linear system is associated physically with the mechanical properties of the hand, arm, and pencil. Since these two samples were written with the same implement, one would expect any discrepancies attributable to physical causes to show up on these samples. Both samples were simulated by using exactly the same settings of the linear system, and both simulations were equally successful. We can conclude from this that the mechanical parameters are not especially significant in the simulation of handwriting, as long as the bound on $\frac{k}{m}$ established in section 3.1 is satisfied. Actually, experiments with the simulator have shown that good simulations can be achieved with $\frac{k}{m}$ values considerably exceeding this bound, but the records in Section II indicate that the parameters associated with most individuals fall well within this bound.

Further evidence of the effect of $\frac{k}{m}$ on handwriting simulation is presented in Fig. 33. Figure 33a shows the result of simulating the record of Fig. 18. Figure 33a and 33c shows the resulting time waveforms. The equivalent value of $\frac{k}{m}$ in this simulation is 3.1.

Figure 33e and 33f shows the time waveforms for the same simulation with an equivalent value of $\frac{k}{m}$ of 0.364. The output of the simulator for this lower value of $\frac{k}{m}$ was the same as for Fig. 33a. Figure 33d shows the input trapezoidal wave for the simulation with $\frac{k}{m} = 3.1$, and Fig. 33g shows the input trapezoidal wave for simulation of the same sample with $\frac{k}{m} = 0.346$. In both of these figures, the top trace is the input to the vertical channel, and the bottom trace is the input to the horizontal channel.

Inspection of Fig. 33 reveals that the timing and amplitude of the trapezoidal input waveforms differ little in the two cases. Adjustments required to compensate for the change in the value of $\frac{k}{m}$ from 3.1 to 0.364 were very minor, but if one examines the

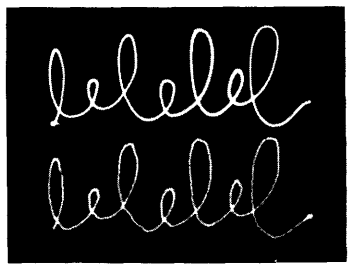

(a)

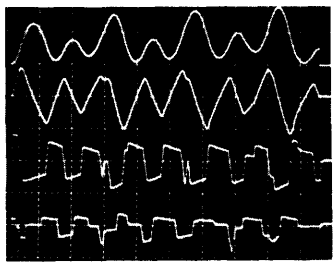

(b)

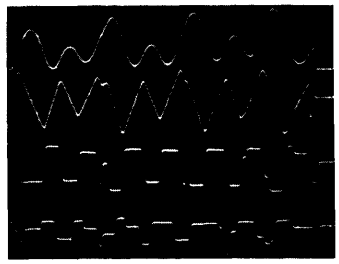

(e)

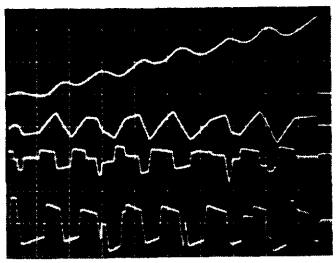

(c)

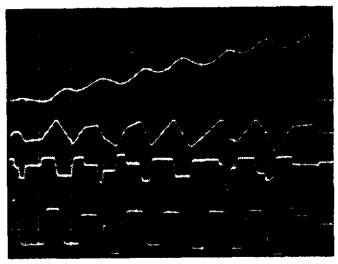

(f)

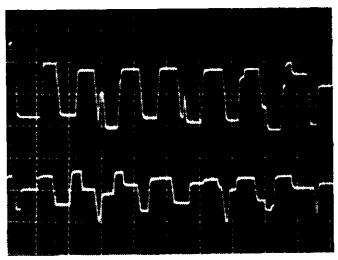

(d)

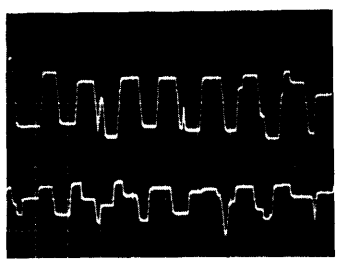

(g)

ALL HORIZONTAL TIME-SCALES 8.5 ms/large division

Fig. 33. Simulation of sample of Fig. 18.

trapezoidal waveform closely, the changes are evident; the amplitudes of the segments tend to be very slightly less in Fig. 33e than the peak amplitudes of Fig. 33b, and the duration of some segments is slightly longer for the larger value of $\frac{k}{m}$. The effect of having a uniform slope on the trapezoidal waves is especially pronounced; compare the negative peaks of v' in Fig. 33 with those of the actual handwriting sample of Fig. 18. Some of these negative peaks are decidedly less rounded than the original. This, of course, is traceable to a much steeper slope in the trapezoidal acceleration waveforms of the simulation at those points.

3.5 SUMMARY

We have presented a description of the handwriting simulator and its operation, together with some examples of its output. We have shown that the use of a multi-level trapezoidal wave enables us to achieve very good duplication of handwriting signals.

One can gain some idea of the accuracy of the simulator insofar as its ability to reproduce handwriting waveforms is concerned from Fig. 34. Figure 34a shows the displacement, velocity, and acceleration of the vertical projection of the word "fell" written by a subject. The simulated version appears in Fig. 34b superimposed upon the image of Fig. 34a. In this simulation,

$$\frac{k}{m} = 1.14$$

which is well within the bound of 1.81 set by inequality (6) for this sample.

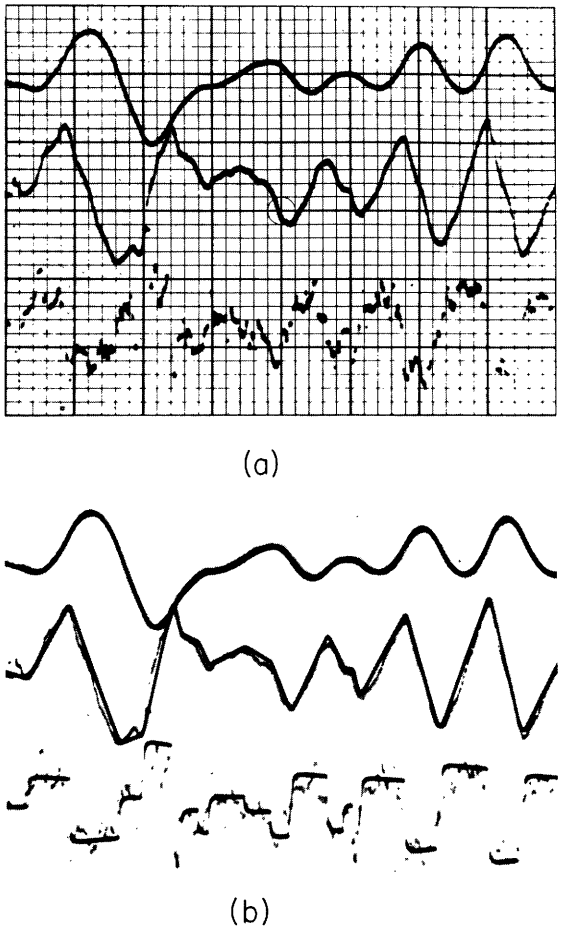

Fig. 34. Accuracy of the simulator.

Matching of displacement is within a linewidth, and the match of velocities is nearly as good. The example of Fig. 34 is typical of many matchings which have been carried out with different words and different subjects. All show the excellent reproduction that the simulator achieves.

The samples just displayed are simulations of the actual samples taken as described in Section II. They show the result of varying $\frac{k}{m}$ over the range of the bound established for this quantity in section 3.1, and illustrate the fact that the effect of $\frac{k}{m}$ on the settings of the

trapezoidal-wave parameters is small. We have also seen that linear systems with widely different ratios of $\frac{k}{m}$ (including zero) can be caused to have matching outputs through adjustment of their inputs.

IV. MODELS FOR THE GENERATION OF HANDWRITING

4.1 A MODEL DERIVED FROM THE EXPERIMENTAL RESULTS

The results presented in Sections II and III have shown that uninterrupted handwriting curves are very closely approximated by signals generated by the simulator described in Section III, and that the velocities and accelerations of handwriting movements are very similar to the first and second derivatives of the simulator output. Thus it is apparent that the differential equation

$$m \frac{d^2x}{dt^2} + k \frac{dx}{dt} = f(t), \tag{7}$$

where f(t) is a trapezoidal time function, provides an output that corresponds closely to that of handwriting movements, and that the velocities and accelerations of the handwriting signal coincide closely with those derived from this simple system. The significant parameter in this equation is the ratio $\frac{k}{m}$. It has been shown in Section III that insofar as simulation of handwriting is concerned, wide tolerance on the value of $\frac{k}{m}$ is acceptable. One can measure its value from the droop of the flat tops of the acceleration waveform. The records of acceleration presented in Section II show considerable noise, as would be expected. No significant droop is observable in these waveforms. Zero droop corresponds to $\frac{k}{m} = 0$, and this is quite unreasonable on physical grounds, since it implies a lossless system! The noise on the acceleration waveform is such that it would mask a small droop. For this reason, we can only set an upper bound on $\frac{k}{m}$. The upper bound set in Section III was such that the droop be less than 25% of the total height of the longest segment of the trapezoidal wave in the sample under consideration. This bound is very conservative, and it is felt that the amount of droop is considerably less than this. An upper bound of 25% on the droop is, however, all that one can safely conclude from the records in Section II alone. This leads to a bound on $\frac{k}{m}$ given by

$$\frac{k}{m} \leq \frac{0.29}{T}, \tag{8}$$

where T is the duration of the longest segment of the trapezoidal wave measured in seconds.

The differential equation (7) is that of a point mass possessing some viscous friction and acted upon by a force. Thus a suitable model, stated in physical terms, is a point mass acted upon by a force that is a trapezoidal time function and may pull in any direction upon the mass during a single segment of the trapezoidal function. The trapezoidal waves generated by the simulator represent the vertical and horizontal projections of the total "force." An illustration of this model is presented in Fig. 35. Figure 35a shows a point mass of parameters m, k acted upon by a force f which is decomposed into its x and y components. Figure 35b shows a point mass acted upon

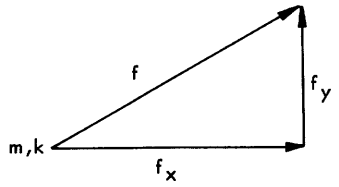

(a)

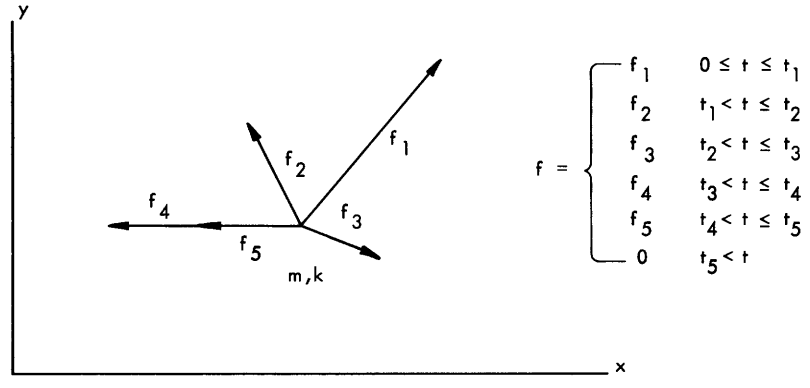

(b)

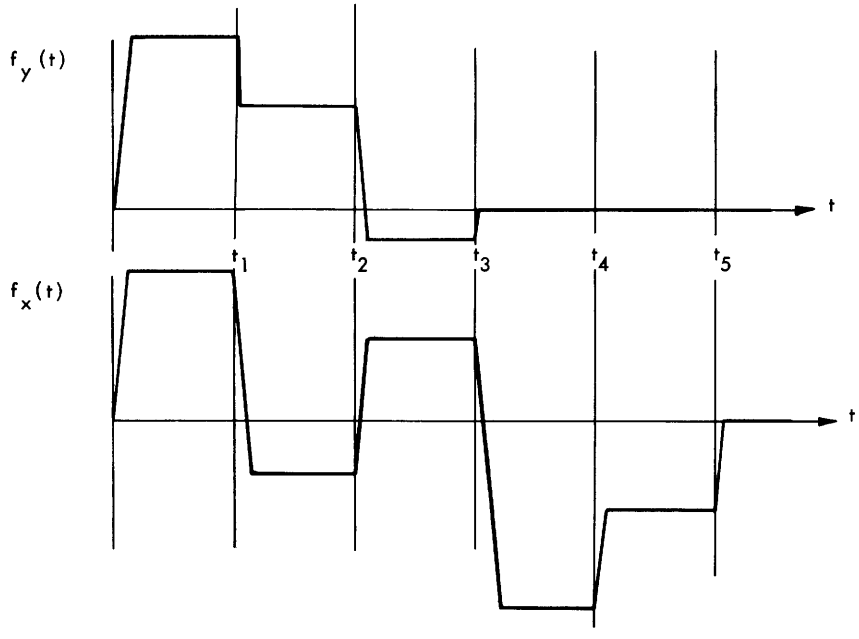

(c)

Fig. 35. Illustration of the model.

by a time-variant force which assumes 5 different vectoral values. No attempt is made to show the motion that would result. The x and y projections of the force waveform are displayed in Fig. 35c.

It is significant to note that we make no statement concerning the existence of independently controlled directions of motion. Some subjects seem to write with two sets of muscles, which cause motion predominantly in two nearly perpendicular directions; while others do not. Thus the supposition of independent directions appears to apply only in particular cases and is not true in general. In this report, we deal only with the projections of the acceleration waveforms on a convenient set of axes. The axes chosen, in most cases, are oriented horizontally and vertically with respect to the writing line. These axes have the virtue of having a simple and direct relationship to the writing itself. As one moves his hand across the page while writing, the directions of action of his musculature on the pencil change with respect to the chosen axes.

Static friction has been neglected in the model of Fig. 35; however, since its effect is readily discernible in the experimental records in Section II, it is necessary to treat its inclusion in the model here. The effect of static friction can be included explicitly simply by inserting a static-friction spike in the force waveform of the simulator when setting it up. To include it implicitly, one must sense the occurrence of zero velocity in both projections simultaneously, and apply the appropriate modification to the "force" waveform. Mathematically, this can be expressed as follows:

$$\left.\begin{aligned} m_x \frac{d^2x}{dt^2} + k_x \frac{dx}{dt} &= f_x(t) - f_{sx}\left[\frac{dx}{dt}, \frac{dy}{dt}\right] \\ m_y \frac{d^2y}{dt^2} + k_y \frac{dy}{dt} &= f_y(t) - f_{sy}\left[\frac{dx}{dt}, \frac{dy}{dt}\right] \end{aligned}\right\} \qquad (9)$$

where $f_{sx}(x',y')$ has the form shown in Fig. 36a, and f_{sy} has the form shown in Fig. 36b. In these figures, the static friction force has zero value except when both velocities are within a small region of width, Δ, about zero.

Equations 9 represent a slightly more exact model for handwriting than Eq. 8 in that the effect of static friction is included. The simulator of Section III does not include this refinement, and static friction is ignored in all of the simulations reported in this work.

4.2 INTERPRETATION OF THE MODEL

The model presented here is based upon the results of the measurements and simulations described in Sections II and III. It is apparent that the output signals predicted by the model match very closely with those observed in actual handwriting.

Because the results upon which the model is based are measurements only of the output of the biological system, we can infer very little from them about the internal functioning of that system. We have seen that the acceleration waveforms of handwriting are approximately trapezoidal. If the physical system that is being accelerated can be

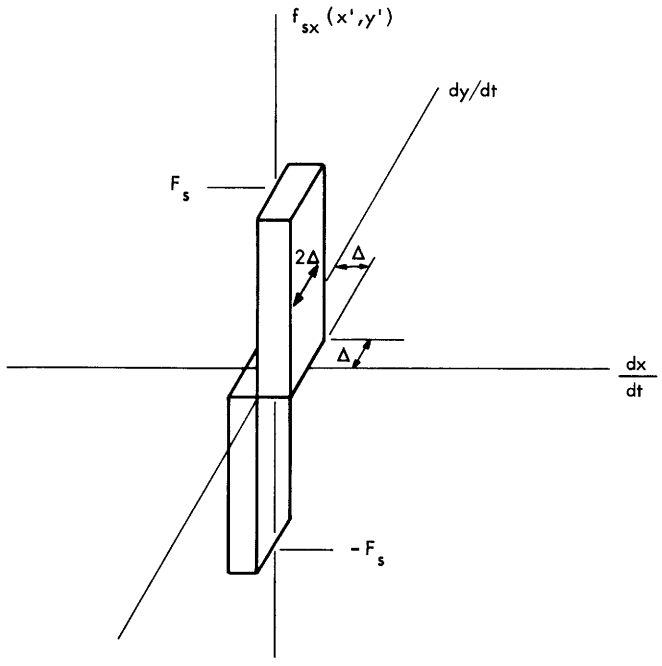

(a)

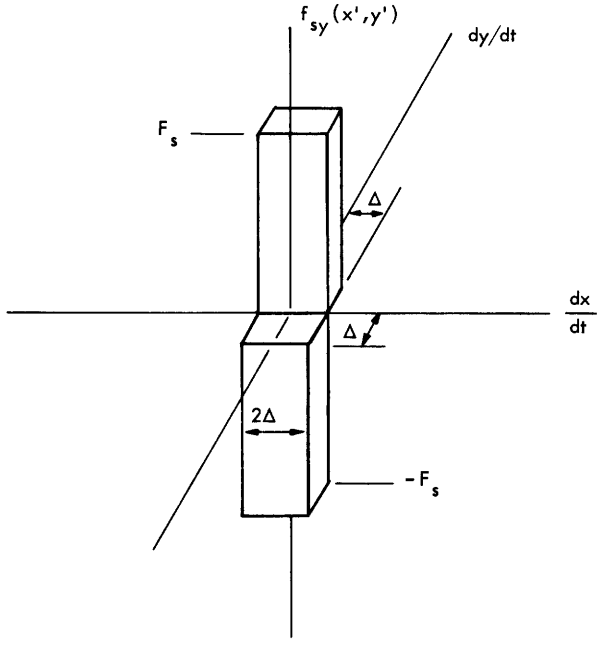

(b)

Fig. 36. Force functions for simulation of static friction.

considered as a lumped system, then the force function giving rise to the acceleration is also trapezoidal. The hand, arm, etc., which is the biological system responsible for handwriting, is a mixture of lumped and distributed parameter systems. It is also active and nonlinear. To what extent it can be represented by a lumped linear system is a question that cannot be answered fully at this time.

If one can consider the biological system to be a lumped one, then the resultant force function causing the acceleration is trapezoidal. But this resultant is composed of a very complex combination of muscle forces, and it is not necessary for these forces to be trapezoidal in order to have a trapezoidal resultant.

The rises and falls of the acceleration are directly attributable to changes in activity in the musculature responsible for them. Thus the zero crossings of the acceleration waveforms are useful for determining timing properties of the biological system.

4.3 SPECULATIONS CONCERNING THE CONTROL OF HANDWRITING

It has already been pointed out that one can say very little about the control of a process by simply examining the output signal. In fact, about all that can be said about the control of handwriting from the measurements described in Section II is that the applied force is approximately constant over short intervals of time, and that it changes abruptly between these intervals, i.e., the force waveform is trapezoidal. In spite of this, experience with the simulator and observation of handwriting signals enables one to make speculations which, though unsupported by direct experiment, are consistent with the observed results.

Denier van der Gon has suggested[1] that the control of handwriting is accomplished by a "pre-set" sequence of signals which control the amplitude and timing of the force waveform (see Fig. 37). The simulator described in Section III is controlled in this fashion. In using the simulator, it was found that very slight perturbations in the "force" waveform in the initial portion of the writing sequence cause catastrophic changes in the rest of the sequence. This is illustrated in Fig. 38. In this figure, the word "bell" as shown in Fig. 38a was set up on the simulator. The time waveforms shown are vertical and horizontal "displacement" and "force." The result displayed in Fig. 38b resulted when a small spike (such as might be caused by an obstruction on the writing surface) was introduced in the first segment of both the horizontal and vertical force signals. In Fig. 38c, the amplitude of one of the initial segments of the vertical waveform was altered slightly. The reason for the lasting effect of these small changes

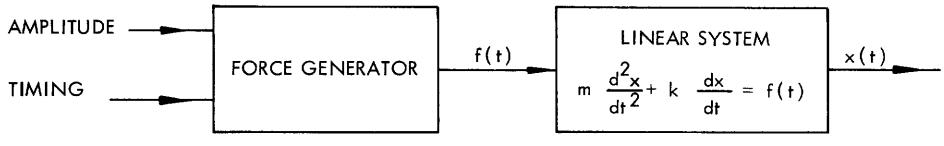

Fig. 37. Model represented by the simulator.

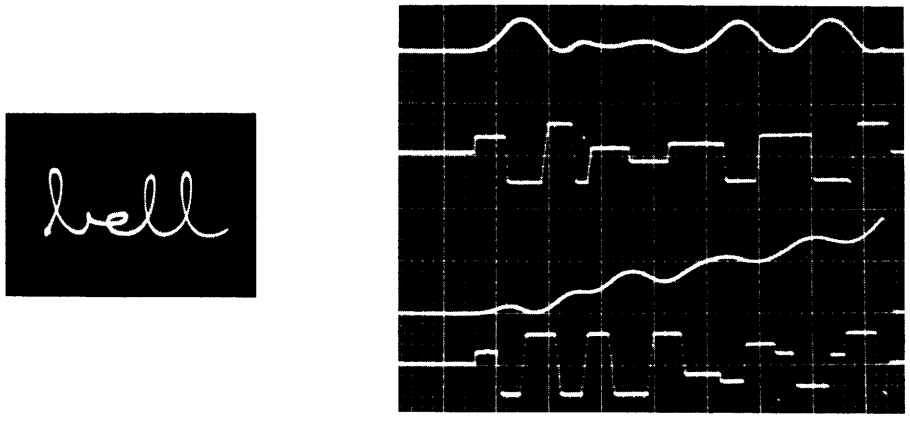

(a)

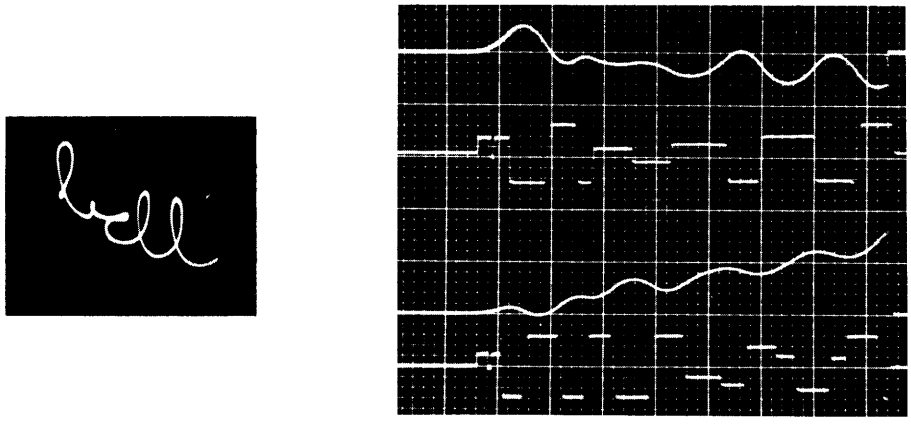

(b)

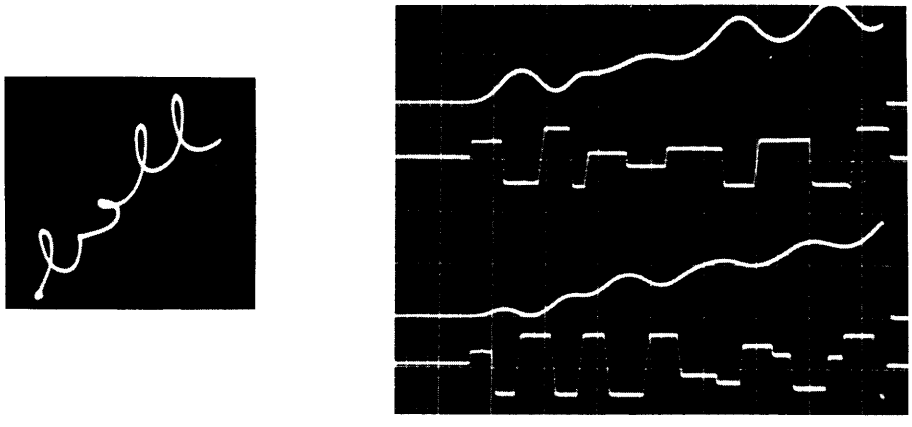

(c)

Fig. 38. Effect of small errors on model of Fig. 37.

is simply the long memory possessed by the system because of its low damping.

A system having the same output as the system of Fig. 37, but which is not as sensitive to perturbations of its outputs, is shown in Fig. 39a. In this system, the inputs are amplitude of force, and the displacement at which this force is required to change. Figure 39b illustrates operation of this system. In this figure, the force level F_1 is generated by the force generator. The resulting displacement is as shown. Sometime before the instant t_1, the level F_2 is preset into the force generator. When the displacement reaches point A, the threshold detector, which has level A as its input, causes the force generator to switch from F_1 to F_2. Note that fixed delay in the feedback loop can be accommodated by this system simply by setting level B, say, into the threshold detector. In this case the delay time Δ would have elapsed before the force changed, at which time the displacement would be at level A, as required.

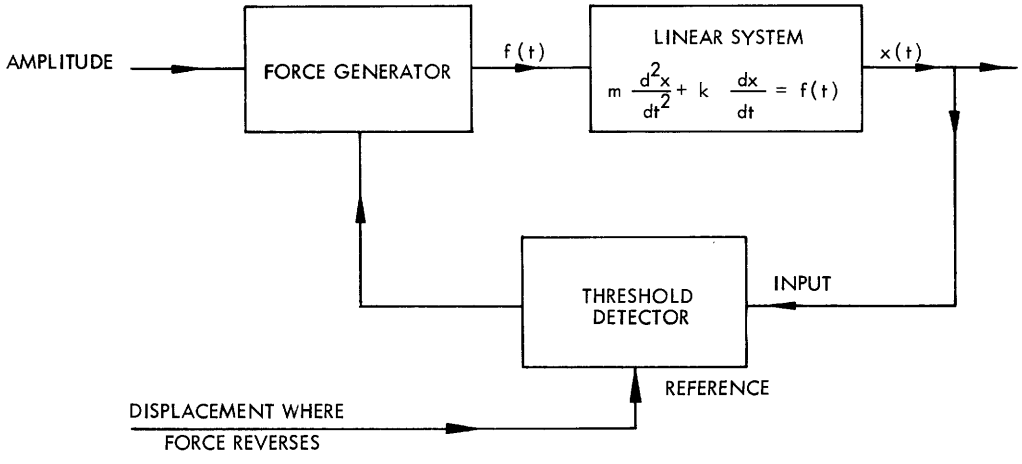

(a)

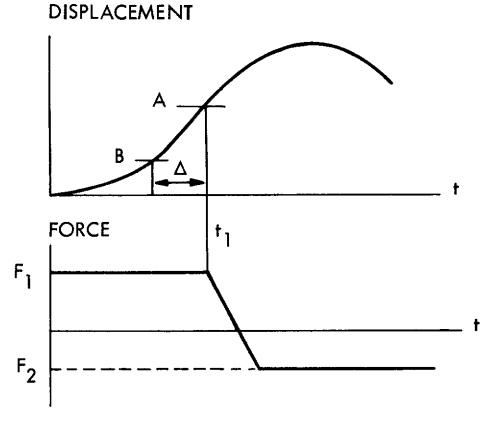

(b)

Fig. 39. A second model.

Experiments recently reported by Denier van der Gon[2] support the validity of the control system of Fig. 39. In his experiment, Denier van der Gon increased the friction between the pencil and the writing surface suddenly and unexpectedly by means of increased magnetic attraction between the two, while a subject was executing the cursive sequence *llllll* . The influence of this friction increase was to cause the amplitude of the writing to decrease while the writing line, however, was held constant. That is, the base line of the sequence of *l*'s was essentially a straight line. It was also reported that there was no appreciable change in the time required to execute an *l* when increased friction was present.

It is difficult to simulate this experiment in two dimensions because of the necessity of ensuring that the friction force be directed tangentially to the instantaneous direction of motion. It is a simple matter, however, to simulate suddenly applied sliding friction in one dimension. The block diagram of the required system appears in Fig. 40.

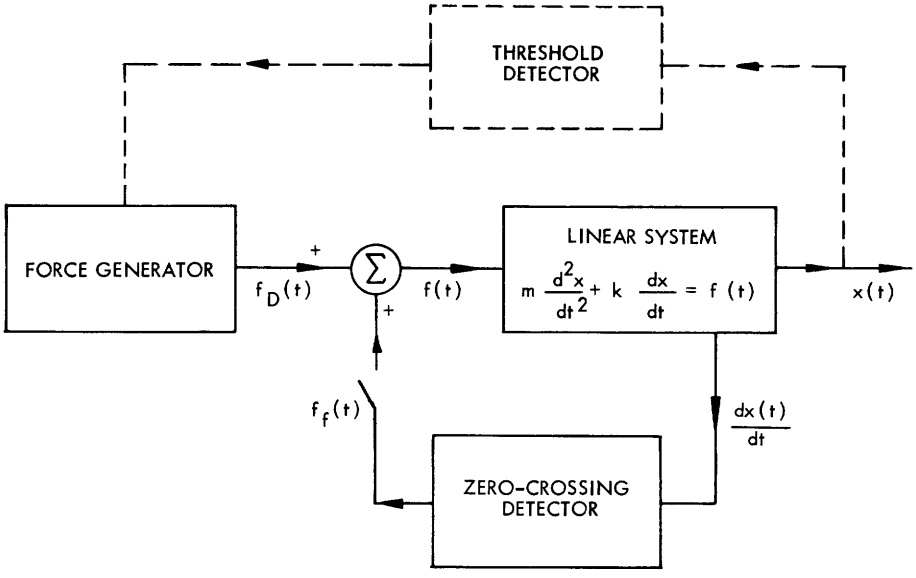

Fig. 40
Diagram for simulation of sliding friction.

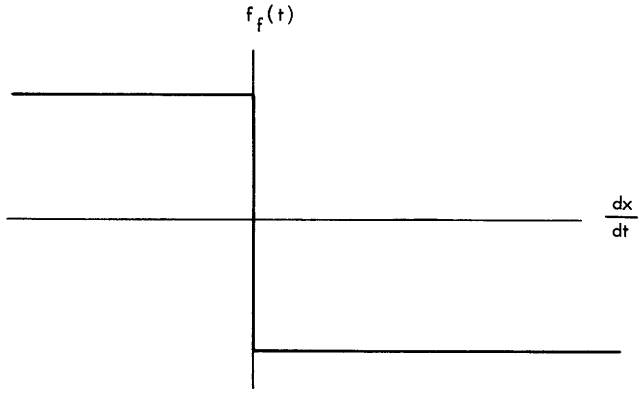

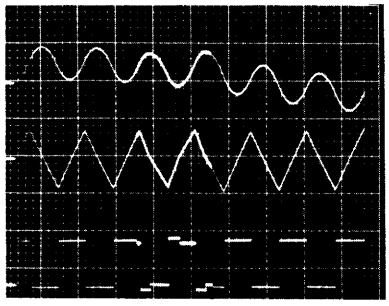

(a)

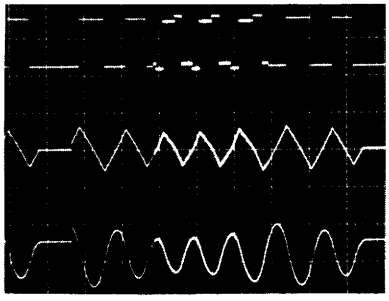

(b)

Fig. 41. Results of sudden increase in friction upon (a) the system of Fig. 37. (b) the system of Fig. 39.

Figure 41a shows the resulting displacement, velocity, and force as functions of time when sliding friction is suddenly applied to the open-loop system of Fig. 37. In Fig. 41a, the increased friction is present during the brightened portion of the waveforms. Figure 41b shows the same set of waveforms when increased friction is applied to the system of Fig. 39. In both of these simulations, the force caused by increased friction is 10% of the driving force.

In the result of Fig. 41a, the effect of increased friction is not so much to decrease its size as to distort the base line. It is also interesting to note that the degree of "bending" of the base line and whether it bends up or down is dependent upon when the increased friction is applied. The system of Fig. 39, however, exhibits behavior more similar to that observed by Denier van der Gon in handwriting. There the base line remains straight, and there is a significant decrease in size. It is also interesting to note that there is only a small decrease in the period of the displacement waveform.

The system of Fig. 39, which has some local feedback, thus is seen to fit the data better than that of Fig. 37. Both systems have identical output waveforms, and are therefore equivalent insofar as their ability to match the measured waveforms of Section II is concerned. Biological mechanisms capable of providing the kind of local feedback required are well known.[17,19] The fact that the proposed system will function with fixed delay in the feedback loop allows for the delay present in nerve signal propagation. The principle of local feedback is also consistent with Lashley's measurements on accuracy of movement.[9]

4.4 SUMMARY

The conclusions to be drawn are that handwriting signals are quite well duplicated by a model consisting of a point mass with slight friction driven by a trapezoidal force function.

Questions concerning the organization of the nervous system which controls handwriting are not covered by this model. The model developed simply describes a system whose output is equivalent to handwriting insofar as the displacement, velocity, and acceleration of the movement are concerned. No conclusions can be drawn concerning the origin of handwriting signals by consideration of this model alone, other than to say that there appears to be a relation of unknown nature between the actual muscle forces

and the "force" signals in the model. Some preliminary results indicate that local feedback may be present, and that the trapezoidal "force" signals can be derived by discrete preset information concerning position and force magnitude. These concepts are in agreement with the experiments of Denier van der Gon[1,2] and Lashley.[9,10]

The model in its present form is very useful for imitating handwriting with a view to establishing the necessary invariants to characterize it. It also provides a basis for further work directed toward studying its relationship with the biological system. The model is also useful for studying the differences and similarities in various styles of handwriting through simulation. Further details on application of the model are to be found in Section V.

V. SUMMARY OF THE WORK: POSSIBLE APPLICATIONS AND EXTENSIONS

5.1 INTRODUCTION

We shall now give a summary of the work and consider some experiments that constitute an initial step in the endeavor to establish relationships between the observed acceleration waveforms and the functional principles of the biological system producing them. Related to this objective is that of determining correspondences between the input to the simulator (i.e., the model) and the inputs to the biological system. It has already been pointed out (Section I) that the present report does not answer questions concerning relations between the measured signals and the functional principles of the organism that gave rise to them. The experiments described here are directed toward that end, and although they are not extensive enough to achieve it, they do indicate a direction of pursuit based upon the results of previous sections.

5.2 ELECTROMYOGRAMS OF MUSCLE PATTERNS DURING HANDWRITING MOVEMENTS

In an effort to gain some knowledge of muscle activity during writing movements, some electromyographic (EMG) records were taken of muscle activity in the forearm and hand. The results appear in Figs. 42 and 43.

Figure 42 is a record of signals made by simple vertical motion. The top and bottom traces are EMG's taken from surface electrodes. The electrodes responsible for the top trace (1) were placed on the palm of the hand, directly over the abductor pollicis brevis at the base of the thumb. The electrodes responsible for the bottom trace (3) were placed on the dorsal part of the forearm, approximately 4 inches below the elbow. The superficial muscles contributing to this signal would be the extensor carpi ulnaris and the extensor digitorum. The center trace (2) is the vertical acceleration signal. Several features of these signals are worthy of note: (i) The EMG signals are remarkably segmented, which gives strong support to the assumption made in Section IV that the controlling force waveform is discrete in nature. (ii) The onset of activity in the EMG signals coincides very well with changes in the slope of the acceleration waveform. Several of these are marked in the figure. The cessation of EMG activity also coincides with reproducible, recognizable features of the acceleration waveform.

Since the two EMG records present an incomplete picture of muscle activity, there are many features on the acceleration waveform that are not accounted for. Unfortunately, equipment was not available to record more than two EMG's simultaneously.

Figure 43 shows waveforms obtained during actual handwriting. Only one EMG is available here, that from surface electrodes near the extensor carpi ulnaris. The segmented character of the EMG is very evident. It is also interesting to note the

Fig. 42. Electromyographic and acceleration waveforms, simple motion.

increase in background activity in the EMG as the horizontal displacement increases. This is probably due to the contraction of the extensor carpi ulnaris which is necessary to bend the wrist to the right. The motions involved in Fig. 43 are complicated, and an attempt to interpret them in terms of a single EMG would be pointless. The waveforms presented do give strong support to the concept of discrete control of the handwriting process.

The results presented in Figs. 42 and 43 also show the feasibility of recording a complete pattern of muscle activity associated with handwriting movements. There are approximately 30 muscles associated with movement of the multiple joints of the hand alone. These muscles are all interwoven in the hand and forearm, so that the use of needle electrodes will be necessary in order to obtain detailed information concerning motor patterns. Paillard[18] has reported an experiment in which a subject traced a cursive figure while EMG signals were taken from 5 coaxial needle electrodes in different muscles. The resulting signals are segmented, but there is no acceleration signal presented with which to correlate the activity.

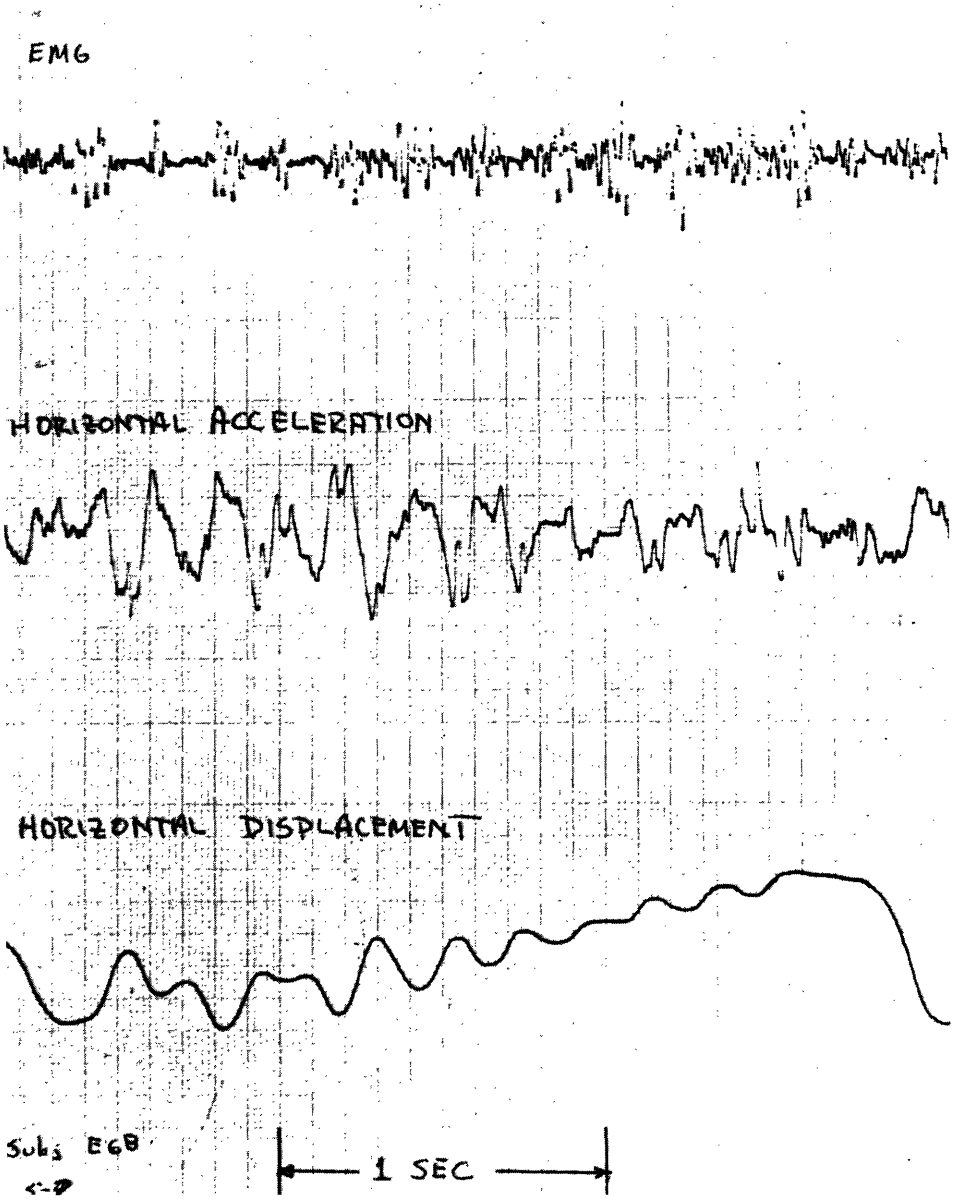

Fig. 43. Electromyographic and acceleration waveforms, handwriting.

5.3 CONTROL OF SIZE OF HANDWRITING MOVEMENTS

We now consider some measurements that were made in an effort to determine how, in terms of the model of Section IV, the size of handwriting movements is controlled. Measurements show that both duration and magnitude of acceleration are observed to change when the size of the writing movement is changed, and the change in magnitude is most pronounced.

Consider first the waveforms shown in Fig. 44a. This figure shows the displacement, velocity, and acceleration of a repetitive left-right movement of the hand about the wrist joint. The size of the oscillatory movement was increased abruptly near the middle of the record but the frequency remained approximately the same. This change in size of movement is reflected chiefly by an increase in the magnitude of the acceleration waveform. The durations of all of the positive segments of the acceleration signal are virtually identical, but the duration of the negative segments does tend to increase with the increased size of the movement as evidenced by the difference in length of the two segments which are marked.

Figure 44b shows similar behavior. Displayed is the vertical projection of a sample of "lelele." The difference in the magnitude of the vertical extent of an e and an l is reflected in changes of both magnitude and duration of the corresponding segments of the acceleration waveform. The samples of lelele presented in Figs. 18 and 19 show more tendency toward control of size by duration, but there is also some variation of magnitude in those records.

We conclude from this discussion that the size of handwriting movement is controlled by both magnitude of force and its duration of application, and which one of these predominates depends upon the subject and the type of movement.

5.4 AMPLITUDE DISTRIBUTION OF THE HANDWRITING OF A SINGLE SUBJECT

A preliminary analysis has been performed on the characteristics of the acceleration waveforms of a single subject. The amplitude of each segment of the vertical acceleration waveform was measured. A histogram of the amplitudes of those sections of the trapezoidal wave which reached a definite level was plotted (see Fig. 45a). The sample taken was composed of measurements of 563 levels.

The histogram, shown in Fig. 45b, shows definite peaks that indicate the possibility of quantization of acceleration levels. No conclusions can be drawn from the result presented here because the spacing of the peaks is less than the uncertainty in measurement caused by the noise. Thus it is not clear whether the peaks are due to some properties of the writing sample or to the method of measurement.

There is a strong possibility that analysis of this type could lead to interesting conclusions and increased knowledge of handwriting movements in particular, and of the nervous system in general. Closely related experiments that can be foreseen include the study of many samples of the same word written by the same person. Here, one could improve the signal-to-noise ratio by averaging techniques prominent in the

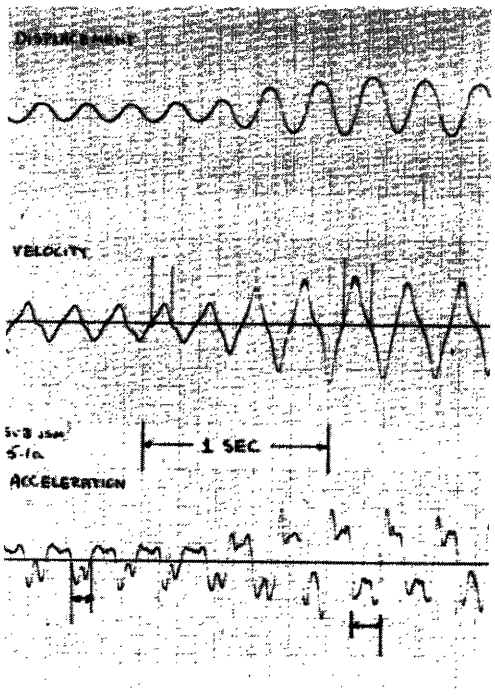

(a)

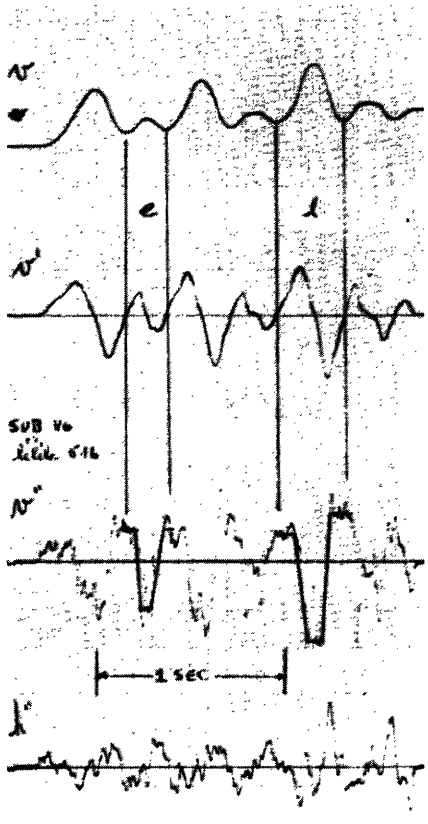

(b)

Fig. 44. Waveforms for changing amplitude of movement.

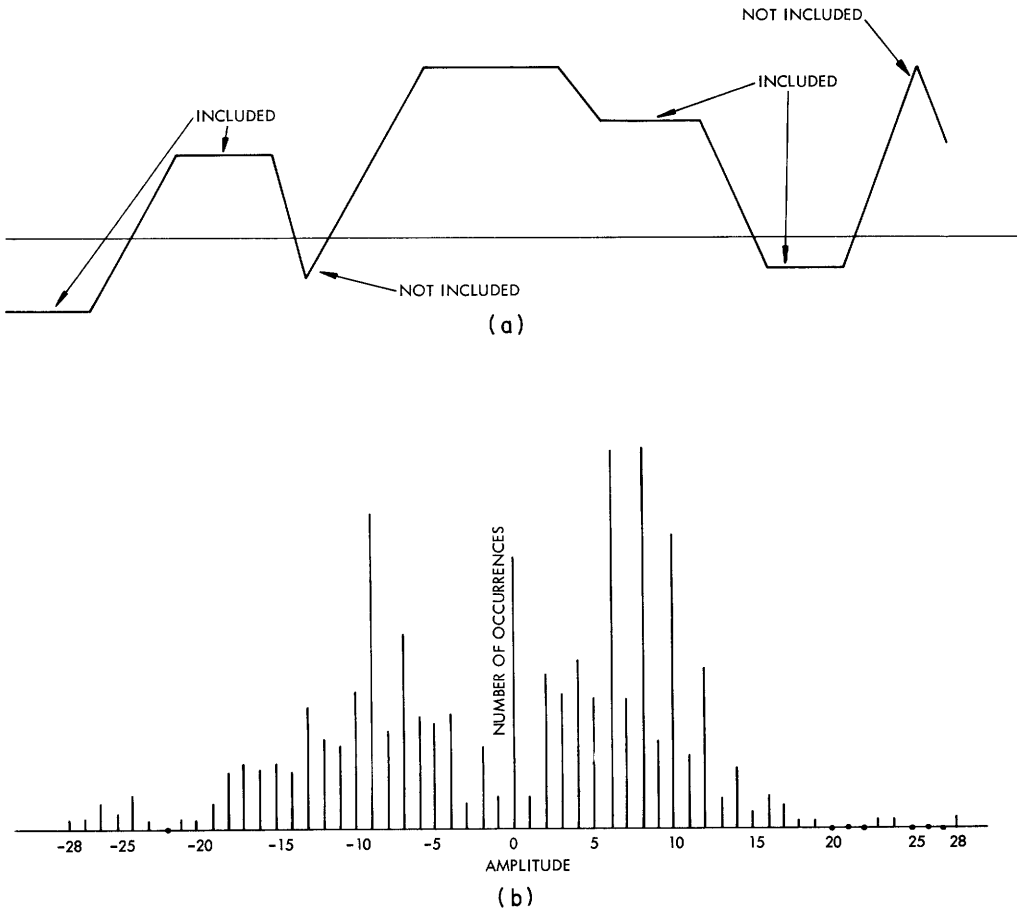

Fig. 45. Histogram of acceleration amplitude, Subject HJZ.

processing of biological signals. The outputs of many averaging processes could then be subjected to the same processing which resulted in the graph of Fig. 45b.

5.5 POSSIBLE APPLICATIONS

There are several possible applications that derive from this work. We shall consider a few of these which seem particularly promising.

5.5.1 Recognition by Machine

Among the means by which man communicates through the written word, handwriting presents the ultimate challenge to automatic recognition of a written or printed message. Unlike printed or typed material, the letters in handwriting are not segmented. Also, they possess a much greater variability of form. Thus not only does one have to face almost infinite variability which necessitates the isolation of invariants* of very general

*The noun 'invariant' is used in this report in the following context: An invariant of a letter (or word) is a property of that letter which is common to all manifestations of it.

character but also one has to solve the segmentation problem on the letter-to-letter level. This combination presents a problem of considerable magnitude.

One possible approach to solving the problem is to study the way in which handwriting is generated. The central idea here is that knowledge about the process by which handwriting is produced may shed some light on means by which it can be recognized. More specifically, there are certain attributes of the output signal (displacement of pencil point) which are due to fixed properties of the system and do not depend on what is being written. These attributes of the signal are irrelevant to the selection of invariants for the purpose of using them to characterize and thus recognize what has been written. Thus if all or some of the properties of the signal which are independent of what is being written can be removed by suitable signal processing, the resulting processed signal may be easier to use in attempting to understand the problem of recognition of handwriting and, in the larger sense, the recognition problem in general. The philosophy of this approach is a variation of the "analysis-by-synthesis" philosophy first proposed for handwriting by Eden and Halle.[4-6]

Recognition procedures for handwriting which to a greater or lesser extent make use of the philosophy of analysis by synthesis are those of Mermelstein[14-16] and Teager.[21] Other important work in the field of handwriting recognition has been done by Frishkopf, Harmon,[8] and Earnest.[3] A comprehensive summary of the field is to be found in a survey article by Lindgren.[11]

In handwriting, the invariants required to identify the content of a sample are present in the acceleration waveform, since the relation between acceleration and displacement is unchanged, irrespective of the movement that is being executed. The possibility exists that the acceleration waveform is more amenable to analysis than the displacement waveform, because of its segmented character. The simulator would be useful in this respect, in that the second derivative of its output closely approximates the acceleration of actual handwriting.

A useful experimental program directed toward the establishment of handwriting invariants would be to study the problems related to the development of a handwriting simulator provided with a set of modules, each of which generates a character. This study would place in evidence such problems as the segmentation of handwriting into letters, the joining of the letters in various sequences, and the possible existence of basic strokes within the framework of the principles of operation of the simulator. The solution of these problems should lead to a set of invariants that characterize the various letters "written" by the simulator. The project would continue by attempting to apply these invariants to the recognition of actual handwriting by machine.

5.5.2 Neurological Studies

The model developed in sections 4.1 and 4.2 and the control systems discussed in section 4.3 imply that the control of handwriting is "preprogrammed," that is, the nerve signals are sent in a predetermined sequence to the muscles according to the action that

is being commanded. There is some evidence of local feedback in the control of these motions, but the supposition at this point in the research is that there is no instantaneous feedback of position information all the way to the brain. This assumption agrees with the results of Lashley[9] who found that accurate motion of the knee joint was possible without any feedback to the brain (spinal injury), provided the motions were rapid. It is possible that further development of the techniques used in this study can clarify some of these matters.

5.6 SUMMARY OF THE PRESENT RESEARCH

Our main concern has been the measurement and interpretation of the acceleration of handwriting and related movements. Because these measurements are made externally on a system whose inputs are unknown, it is not possible to draw any definite conclusions about the control of the handwriting process, other than to say that it is almost certainly discrete in nature. Some speculations have been advanced concerning the control of the process which are consistent with physiological knowledge, the present measurements, and what would be required of a control system to perform tasks such as handwriting.

Acknowledgment

It is a genuine pleasure to thank Dr. Manuel V. Cerrillo for teaching me how to use and expand the knowledge gained through ten years of higher education. His influence has broadened my professional horizons immeasurably. Special thanks are due to Professor Henry J. Zimmermann for his interest, encouragement, suggestions, and constructive criticism during the course of this work. I am also grateful for the contributions made through helpful suggestions and criticisms by Professor Amar G. Bose, Dr. Jerome Y. Lettvin, Professor Samuel J. Mason, and Dr. Warren S. McCulloch.

The technical assistance of the Research Laboratory of Electronics research staff, particularly Mr. E. G. Banks, Mr. H. J. Lander, and Miss Judi Sahagen, is gratefully acknowledged.

References

1. J. J. Denier van der Gon, J. Ph. Thuring, and J. Strackee, "A Handwriting Simulator," Physics in Medicine and Biology, Vol. 6, No. 3, pp. 407-414, January 1962.
2. J. J. Denier van der Gon and J. Ph. Thuring, "The Guiding of Human Writing Movements," Kybernetic, Band II, Heft 4, February 1965, pp. 145-148.
3. L. D. Earnest, "Machine Recognition of Cursive Writing," in Information Processing 1962, Proc. IFIP Congress 62, C. M. Popplewell (ed.) (Amsterdam, North-Holland Publishing Co., 1963), pp. 462-466.
4. M. Eden and M. Halle, "Characterization of Cursive Writing," Quarterly Progress Report No. 55, Research Laboratory of Electronics, M. I. T., October 15, 1959, pp. 152-156.
5. M. Eden and M. Halle, "The Characterization of Cursive Writing," Fourth London Symposium on Information Theory, C. Cherry (ed.) (Butterworths, Washington, D.C., 1961), pp. 287-298.
6. M. Eden, "Handwriting and Pattern Recognition," IRE Trans., Vol. IT-8, No. 2, 1962, pp. 160-166.
7. P. A. Einstein, "Factors Limiting the Accuracy of Electrolytic Plotting Tanks," Brit. J. Appl. Physics, Vol. 2, pp. 49-55, 1951.
8. L. S. Frishkopf and L. D. Harmon, "Machine Recognition of Cursive Script," Fourth London Symposium on Information Theory, C. Cherry (ed.) (Butterworths, London, 1961), pp. 300-315.
9. K. S. Lashley, "The Accuracy of Movement in the Absence of Excitation from the Moving Organ," Am. J. Physiol., Vol. 43, pp. 169-194, 1917.
10. K. S. Lashley, "Cerebral Mechanism in Behavior," The Hixon Symposium, L. A. Jeffress (ed.) (New York, John Wiley and Sons, Inc., 1951), pp. 112-136.
11. N. Lindgren, "Machine Recognition of Human Language, Part III – Cursive Script Recognition," IEEE Spectrum, May 1965, pp. 104-116.
12. J. S. MacDonald, "Experimental Studies of Handwriting Signals," Ph.D. Thesis, Department of Electrical Engineering, M. I. T., August 1964.
13. J. S. MacDonald, "Rectangular Wave Generator," Quarterly Progress Report No. 73 Research Laboratory of Electronics, M. I. T., April 15, 1964, pp. 135-139.
14. P. Mermelstein, "Computer Recognition of Connected Handwritten Words," Sc.D. Thesis, Department of Electrical Engineering, M. I. T., January 1964.
15. P. Mermelstein and M. Eden, "A System for Automatic Recognition of Handwritten Words," Proc. Fall Joint Computer Conference, 1964, pp. 333-342.
16. P. Mermelstein and M. Eden, "Experiments on Computer Recognition of Connected Handwritten Words," Inform Contr., Vol. 7, No. 2, June 1964, pp. 255-270.
17. P. A. Merton, "Speculations on the Servo-Control of Movement," CIBA Symposium, The Spinal Cord, pp. 247-260.
18. J. Paillard, "The Patterning of Skilled Movements," in Handbook of Physiology, Section 1, Neurophysiology, Vol. III, J. Field, H. W. Magaun, V. E. Hall (eds.) (American Physiological Society), p. 1684.
19. S. Skogland, "Anatomical and Physiological Studies of Knee Joint Innervation in the Cat," Acta Physiol. Scandinav., Vol. 36, Suppl. 124, 1956.
20. M. O. J. Smith, "Nonlinear Computations in the Human Controller," IRE Trans., Vol. BME-9, pp. 125-128, April 1962.
21. H. M. Teager, "Multidimensional Visual Information Processing," in Advances in Biomedical Computer Applications (New York Academy of Sciences, 1965, in press).

JOINT SERVICES ELECTRONICS PROGRAM
REPORTS DISTRIBUTION LIST

Department of Defense

Dr. Edward M. Reilley
Asst Director (Research)
Ofc of Defense Res & Eng
Department of Defense
Washington, D.C. 20301

Office of Deputy Director
(Research and Information Room 3D1037)
Department of Defense
The Pentagon
Washington, D.C. 20301

Director
Advanced Research Projects Agency
Department of Defense
Washington, D.C. 20301

Director for Materials Sciences
Advanced Research Projects Agency
Department of Defense
Washington, D.C. 20301

Headquarters
Defense Communications Agency (333)
The Pentagon
Washington, D.C. 20305

Defense Documentation Center
Attn: TISIA
Cameron Station, Bldg. 5
Alexandria, Virginia 22314

Director
National Security Agency
Attn: Librarian C-332
Fort George G. Meade, Maryland 20755

Weapons Systems Evaluation Group
Attn: Col. Finis G. Johnson
Department of Defense
Washington, D.C. 20305

National Security Agency
Attn: R4-James Tippet
Office of Research
Fort George G. Meade, Maryland 20755

Central Intelligence Agency
Attn: OCR/DD Publications
Washington, D.C. 20505

Department of the Air Force

AUL3T-9663
Maxwell AFB, Alabama 36112

AFRSTE
Hqs. USAF
Room ID-429, The Pentagon
Washington, D.C. 20330

AFFTC (FTBPP-2)
Technical Library
Edwards AFB, Calif. 93523

Space Systems Division
Air Force Systems Command
Los Angeles Air Force Station
Los Angeles, California 90045
Attn: SSSD

SSD(SSTRT/Lt. Starbuck)
AFUPO
Los Angeles, California 90045

Det #6, OAR (LOOAR)
Air Force Unit Post Office
Los Angeles, California 90045

Systems Engineering Group (RTD)
Technical Information Reference Branch
Attn: SEPIR
Directorate of Engineering Standards
and Technical Information
Wright-Patterson AFB, Ohio 45433

ARL (ARIY)
Wright-Patterson AFB, Ohio 45433

AFAL (AVT)
Wright-Patterson AFB, Ohio 45433

AFAL (AVTE/R. D. Larson)
Wright-Patterson AFB, Ohio 45433

Office of Research Analyses
Attn: Technical Library Branch
Holloman AFB, New Mexico 88330

Commanding General
Attn: STEWS-WS-VT
White Sands Missile Range
New Mexico 88002

RADC (EMLAL-1)
Griffiss AFB, New York 13442
Attn: Documents Library

AFCRL (CRMXLR)
AFCRL Research Library, Stop 29
L. G. Hanscom Field
Bedford, Massachusetts 01731

Academy Library DFSLB)
U.S. Air Force Academy
Colorado 80840

FJSRL
USAF Academy, Colorado 80840

APGC (PGBPS-12)
Eglin AFB, Florida 32542

AFETR Technical Library
(ETV, MU-135)
Patrick AFB, Florida 32925

AFETR (ETLLG-1)
STINFO Officer (for Library)
Patrick AFB, Florida 32925

ESD (ESTI)
L. G. Hanscom Field
Bedford, Massachusetts 01731

AEDC (ARO, INC)
Attn: Library/Documents
Arnold AFS, Tennessee 37389

European Office of Aerospace Research
Shell Building
47 Rue Cantersteen
Brussels, Belgium

Lt. Col. E. P. Gaines, Jr.
Chief, Electronics Division
Directorate of Engineering Sciences
Air Force Office of Scientific Research
Washington, D.C. 20333

Department of the Army

U.S. Army Research Office
Attn: Physical Sciences Division
3045 Columbia Pike
Arlington, Virginia 22204

Research Plans Office
U.S. Army Research Office
3045 Columbia Pike
Arlington, Virginia 22204

Commanding General
U.S. Army Materiel Command
Attn: AMCRD-RS-PE-E
Washington, D.C. 20315

Commanding General
U.S. Army Strategic Communications
Command
Washington, D.C. 20315

Commanding Officer
U.S. Army Materials Research Agency
Watertown Arsenal
Watertown, Massachusetts 02172

Commanding Officer
U.S. Army Ballistics Research Laboratory
Attn: V. W. Richards
Aberdeen Proving Ground
Aberdeen, Maryland 21005

Commandant
U.S. Army Air Defense School
Attn: Missile Sciences Division C&S Dept.
P.O. Box 9390
Fort Bliss, Texas 79916

Commanding General
Frankford Arsenal
Attn: SMUFA-L6000 (Dr. Sidney Ross)
Philadelphia, Pennsylvania 19137

Commanding General
U.S. Army Missile Command
Attn: Technical Library
Redstone Arsenal, Alabama 35809

U.S. Army Munitions Command
Attn: Technical Information Branch
Picatinney Arsenal
Dover, New Jersey 07801

Commanding Officer
Harry Diamond Laboratories
Attn: Mr. Berthold Altman
Connecticut Avenue and Van Ness St. N.W.
Washington, D.C. 20438

Commanding Officer
U.S. Army Security Agency
Arlington Hall
Arlington, Virginia 22212

Commanding Officer
U.S. Army Limited War Laboratory
Attn: Technical Director
Aberdeen Proving Ground
Aberdeen, Maryland 21005

Commanding Officer
Human Engineering Laboratories
Aberdeen Proving Ground, Maryland 21005

Director
U.S. Army Engineer
Geodesy, Intelligence and Mapping
Research and Development Agency
Fort Belvoir, Virginia 22060

Commandant
U.S. Army Command and General
Staff College
Attn: Secretary
Fort Leavenworth, Kansas 66270

Dr. H. Robl, Deputy Chief Scientist
U.S. Army Research Office (Durham)
Box CM, Duke Station
Durham, North Carolina 27706

Commanding Officer
U.S. Army Research Office (Durham)
Attn: CRD-AA-IP (Richard O. Ulsh)
Box CM, Duke Station
Durham, North Carolina 27706

Superintendent
U.S. Army Military Academy
West Point, New York 10996

The Walter Reed Institute of Research
Walter Reed Medical Center
Washington, D.C. 20012

Commanding Officer
U.S. Army Engineer R&D Laboratory
Attn: STINFO Branch
Fort Belvoir, Virginia 22060

Commanding Officer
U.S. Army Electronics R&D Activity
White Sands Missile Range,
New Mexico 88002

Dr. S. Benedict Levin, Director
Institute for Exploratory Research
U.S. Army Electronics Command
Attn: Mr. Robert O. Parker, Executive
Secretary, JSTAC (AMSEL-XL-D)
Fort Monmouth, New Jersey 07703

Commanding General
U.S. Army Electronics Command
Fort Monmouth, New Jersey 07703
Attn: AMSEL-SC
AMSEL-RD-D
RD-G
RD-MAF-1
RD-MAT
RD-GF
XL-D
XL-E
XL-C
XL-S
HL-D
HL-L
HL-J
HL-P
HL-O
HL-R
NL-D
NL-A
NL-P
NL-R
NL-S
KL-D
KL-E
KL-S
KL-T
VL-D
WL-D

Department of the Navy

Chief of Naval Research
Department of the Navy
Washington, D.C. 20360
Attn: Code 427

Chief, Bureau of Ships
Department of the Navy
Washington, D.C. 20360

Chief, Bureau of Weapons
Department of the Navy
Washington, D.C. 20360

Commanding Officer
Office of Naval Research Branch Office
Box 39, Navy No 100 F.P.O.
New York, New York 09510

Commanding Officer
Office of Naval Research Branch Office
1030 East Green Street
Pasadena, California

Commanding Officer
Office of Naval Research Branch Office
219 South Dearborn Street
Chicago, Illinois 60604

Commanding Officer
Office of Naval Research Branch Office
207 West 42nd Street
New York, New York 10011

Commanding Officer
Office of Naval Research Branch Office
495 Summer Street
Boston, Massachusetts 02210

Director, Naval Research Laboratory
Technical Information Officer
Washington, D.C.
Attn: Code 2000

Commander
Naval Air Development and Material Center
Johnsville, Pennsylvania 18974

Librarian, U.S. Electronics Laboratory
San Diego, California 95152

Commanding Officer and Director
U.S. Naval Underwater Sound Laboratory
Fort Trumbull
New London, Connecticut 06840

Librarian, U.S. Naval Post Graduate School
Monterey, California

Commander
U.S. Naval Air Missile Test Center
Point Magu, California

Director
U.S. Naval Observatory
Washington, D.C.

Chief of Naval Operations
OP-07
Washington, D.C.

Director, U.S. Naval Security Group
Attn: G43
3801 Nebraska Avenue
Washington, D.C.

Commanding Officer
Naval Ordnance Laboratory
White Oak, Maryland

Commanding Officer
Naval Ordnance Laboratory
Corona, California

Commanding Officer
Naval Ordnance Test Station
China Lake, California

Commanding Officer
Naval Avionics Facility
Indianapolis, Indiana

Commanding Officer
Naval Training Device Center
Orlando, Florida

U.S. Naval Weapons Laboratory
Dahlgren, Virginia

Weapons Systems Test Division
Naval Air Test Center
Patuxtent River, Maryland
Attn: Library

Other Government Agencies

Mr. Charles F. Yost
Special Assistant to the Director
of Research
NASA
Washington, D.C. 20546

NASA Lewis Research Center
Attn: Library
21000 Brookpark Road
Cleveland, Ohio 44135

Dr. H. Harrison, Code RRE
Chief, Electrophysics Branch
NASA, Washington, D.C. 20546

Goddard Space Flight Center
NASA
Attn: Library, Documents Section Code 252
Green Belt, Maryland 20771

National Science Foundation
Attn: Dr. John R. Lehmann
Division of Engineering
1800 G Street N.W.
Washington, D.C. 20550

U.S. Atomic Energy Commission
Division of Technical Information Extension
P.O. Box 62
Oak Ridge, Tennessee 37831

Los Alamos Scientific Library
Attn: Reports Library
P.O. Box 1663
Los Alamos, New Mexico 87544

NASA Scientific & Technical Information
Facility
Attn: Acquisitions Branch (S/AK/DL)
P.O. Box 33
College Park, Maryland 20740

Non-Government Agencies

Director
Research Laboratory for Electronics
Massachusetts Institute of Technology
Cambridge, Massachusetts 02139

Polytechnic Institute of Brooklyn
55 Johnson Street
Brooklyn, New York 11201
Attn: Mr. Jerome Fox
Research Coordinator

Director
Columbia Radiation Laboratory
Columbia University
538 West 120th Street
New York, New York 10027

Director
Stanford Electronics Laboratories
Stanford University
Stanford, California

Director
Coordinated Science Laboratory
University of Illinois
Urbana, Illinois 61803

Director
Electronics Research Laboratory
University of California
Berkeley 4, California

Director
Electronics Sciences Laboratory
University of Southern California
Los Angeles, California 90007

Professor A. A. Dougal, Director
Laboratories for Electronics and
Related Sciences Research
University of Texas
Austin, Texas 78712

Division of Engineering and Applied
Physics
210 Pierce Hall
Harvard University
Cambridge, Massachusetts 02138

Aerospace Corporation
P.O. Box 95085
Los Angeles, California 90045
Attn: Library Acquisitions Group

Professor Nicholas George
California Institute of Technology
Pasadena, California

Aeronautics Library
Graduate Aeronautical Laboratories
California Institute of Technology
1201 E. California Blvd.
Pasadena, California 91109

Director, USAF Project RAND
Via: Air Force Liaison Office
The RAND Corporation
1700 Main Street
Santa Monica, California 90406
Attn: Library

The Johns Hopkins University
Applied Physics Laboratory
8621 Georgia Avenue
Silver Spring, Maryland
Attn: Boris W. Kuvshinoff
Document Librarian

School of Engineering Sciences
Arizona State University
Tempe, Arizona

Dr. Leo Young
Stanford Research Institute
Menlo Park, California

Hunt Library
Carnegie Institute of Technology
Schenley Park
Pittsburgh, Pennsylvania 15213

Mr. Henry L. Bachmann
Assistant Chief Engineer
Wheeler Laboratories
122 Cuttermill Road
Great Neck, New York

University of Liege
Electronic Institute
15, Avenue Des Tilleuls
Val-Benoit, Liege
Belgium

University of California at Los Angeles
Department of Engineering
Los Angeles, California

California Institute of Technology
Pasadena, California
Attn: Documents Library

University of California
Santa Barbara, California
Attn: Library

Carnegie Institute of Technology
Electrical Engineering Department
Pittsburgh, Pennsylvania

University of Michigan
Electrical Engineering Department
Ann Arbor, Michigan

New York University
College of Engineering
New York, New York

Syracuse University
Dept. of Electrical Engineering
Syracuse, New York

Yale University
Engineering Department
New Haven, Connecticut

Bendix Pacific Division
11600 Sherman Way
North Hollywood, California

General Electric Company
Research Laboratories
Schenectady, New York

Airborne Instruments Laboratory
Deerpark, New York

Lockheed Aircraft Corporation
P.O. Box 504
Sunnyvale, California

Raytheon Company
Bedford, Massachusetts
Attn: Librarian

UNCLASSIFIED

Security Classification

DOCUMENT CONTROL DATA - R&D

(Security classification of title, body of abstract and indexing annotation must be entered when the overall report is classified)

1. ORIGINATING ACTIVITY (Corporate author) Research Laboratory of Electronics Massachusetts Institute of Technology Cambridge, Massachusetts	2a. REPORT SECURITY CLASSIFICATION Unclassified 2b GROUP None

3. REPORT TITLE

Experimental Studies of Handwriting Signals

4. DESCRIPTIVE NOTES (Type of report and inclusive dates)

Technical Report

5. AUTHOR(S) (Last name, first name, initial)

MacDonald, John S.

6. REPORT DATE	7a. TOTAL NO. OF PAGES	7b. NO. OF REFS
March 31, 1966	76	21

8a. CONTRACT OR GRANT NO.	9a. ORIGINATOR'S REPORT NUMBER(S)
DA36-039-AMC-03200(E) b. PROJECT NO. 200-14501-B31F c. NSF Grant GP-2495 NIH Grant MH-04737-05 d. NASA Grant NsG-496	Technical Report 443 9b. OTHER REPORT NO(S) (Any other numbers that may be assigned this report)

10. AVAILABILITY/LIMITATION NOTICES

Distribution of this document is unlimited

11. SUPPLEMENTARY NOTES	12. SPONSORING MILITARY ACTIVITY
	Joint Services Electronics Program thru USAECOM, Fort Monmouth, N.J.

13. ABSTRACT

A system for measuring the displacement, velocity, and acceleration of handwriting movements has been developed. Samples of handwriting processed by this system indicate that the acceleration waveforms of uninterrupted handwriting approximate multilevel trapezoidal time functions.

Electronic simulation of the measured displacement, velocity, and acceleration waveforms of handwriting has been accomplished. The "handwriting" produced by the electronic simulator can duplicate uninterrupted handwriting with a high degree of accuracy. The simulator has been used both to generate samples of "handwriting" and to duplicate the handwriting of a number of subjects.

The simulator, in effect, represents a point mass driven by a trapezoidal "force" function. Although the biological system producing handwriting is highly complex, the motions involved can be duplicated with a high degree of accuracy in terms of an extremely simple mechanical model.

Some preliminary results have been obtained which are directed toward the establishment of relations between the model and the biological system responsible for handwriting. Possible applications of the techniques and apparatus developed in this report to problems of handwriting recognition and neurological studies are discussed.

DD FORM 1 JAN 64 1473

UNCLASSIFIED

Security Classification

14. KEY WORDS	LINK A		LINK B		LINK C	
	ROLE	WT	ROLE	WT	ROLE	WT
handwriting simulation biophysical measurement simulation of biological processes bionics biophysical models						

INSTRUCTIONS

1. ORIGINATING ACTIVITY: Enter the name and address of the contractor, subcontractor, grantee, Department of Defense activity or other organization *(corporate author)* issuing the report.

2a. REPORT SECURITY CLASSIFICATION: Enter the overall security classification of the report. Indicate whether "Restricted Data" is included. Marking is to be in accordance with appropriate security regulations.

2b. GROUP: Automatic downgrading is specified in DoD Directive 5200.10 and Armed Forces Industrial Manual. Enter the group number. Also, when applicable, show that optional markings have been used for Group 3 and Group 4 as authorized.

3. REPORT TITLE: Enter the complete report title in all capital letters. Titles in all cases should be unclassified. If a meaningful title cannot be selected without classification, show title classification in all capitals in parenthesis immediately following the title.

4. DESCRIPTIVE NOTES: If appropriate, enter the type of report, e.g., interim, progress, summary, annual, or final. Give the inclusive dates when a specific reporting period is covered.

5. AUTHOR(S): Enter the name(s) of author(s) as shown on or in the report. Enter last name, first name, middle initial. If military, show rank and branch of service. The name of the principal author is an absolute minimum requirement.

6. REPORT DATE: Enter the date of the report as day, month, year; or month, year. If more than one date appears on the report, use date of publication.

7a. TOTAL NUMBER OF PAGES: The total page count should follow normal pagination procedures, i.e., enter the number of pages containing information.

7b. NUMBER OF REFERENCES: Enter the total number of references cited in the report.

8a. CONTRACT OR GRANT NUMBER: If appropriate, enter the applicable number of the contract or grant under which the report was written.

8b, 8c, & 8d. PROJECT NUMBER: Enter the appropriate military department identification, such as project number, subproject number, system numbers, task number, etc.

9a. ORIGINATOR'S REPORT NUMBER(S): Enter the official report number by which the document will be identified and controlled by the originating activity. This number must be unique to this report.

9b. OTHER REPORT NUMBER(S): If the report has been assigned any other report numbers *(either by the originator or by the sponsor)*, also enter this number(s).

10. AVAILABILITY/LIMITATION NOTICES: Enter any limitations on further dissemination of the report, other than those imposed by security classification, using standard statements such as:

(1) "Qualified requesters may obtain copies of this report from DDC."

(2) "Foreign announcement and dissemination of this report by DDC is not authorized."

(3) "U. S. Government agencies may obtain copies of this report directly from DDC. Other qualified DDC users shall request through _____."

(4) "U. S. military agencies may obtain copies of this report directly from DDC. Other qualified users shall request through _____."

(5) "All distribution of this report is controlled. Qualified DDC users shall request through _____."

If the report has been furnished to the Office of Technical Services, Department of Commerce, for sale to the public, indicate this fact and enter the price, if known.

11. SUPPLEMENTARY NOTES: Use for additional explanatory notes.

12. SPONSORING MILITARY ACTIVITY: Enter the name of the departmental project office or laboratory sponsoring *(paying for)* the research and development. Include address.

13. ABSTRACT: Enter an abstract giving a brief and factual summary of the document indicative of the report, even though it may also appear elsewhere in the body of the technical report. If additional space is required, a continuation sheet shall be attached.

It is highly desirable that the abstract of classified reports be unclassified. Each paragraph of the abstract shall end with an indication of the military security classification of the information in the paragraph, represented as *(TS), (S), (C), or (U)*

There is no limitation on the length of the abstract. However, the suggested length is from 150 to 225 words.

14. KEY WORDS: Key words are technically meaningful terms or short phrases that characterize a report and may be used as index entries for cataloging the report. Key words must be selected so that no security classification is required. Identifiers, such as equipment model designation, trade name, military project code name, geographic location, may be used as key words but will be followed by an indication of technical context. The assignment of links, rules, and weights is optional.